Spring 2018

Vertical Distribution of Olympia oyster (Ostrea lurida) larvae in Fidalgo Bay, WA

Brooke A. McIntyre
Western Washington University, mcintyba@gmail.com

Vertical Distribution of Olympia oyster (*Ostrea lurida*) larvae in Fidalgo Bay, WA

By

Brooke A. McIntyre

Accepted in Partial Completion
of the Requirements for the Degree
Master of Science

ADVISORY COMMITTEE

Dr. Shawn M. Arellano

Dr. Erika E. McPhee-Shaw

Dr. Brian L. Bingham

Dr. Marco B. A. Hatch

GRADUATE SCHOOL

Dr. Gautam Pillay, Dean

Master's Thesis

In presenting this thesis in partial fulfillment of the requirements for a master's degree at Western Washington University, I grant to Western Washington University the non-exclusive royalty-free right to archive, reproduce, distribute, and display the thesis in any and all forms, including electronic format, via any digital library mechanisms maintained by WWU.

I represent and warrant this is my original work, and does not infringe or violate any rights of others. I warrant that I have obtained written permissions from the owner of any third party copyrighted material included in these files.

I acknowledge that I retain ownership rights to the copyright of this work, including but not limited to the right to use all or part of this work in future works, such as articles or books.

Library users are granted permission for individual, research and non-commercial reproduction of this work for educational purposes only. Any further digital posting of this document requires specific permission from the author.

Any copying or publication of this thesis for commercial purposes, or for financial gain, is not allowed without my written permission.

Brooke McIntyre

May 18, 2018

Vertical Distribution of Olympia oyster (*Ostrea lurida*) larvae in Fidalgo Bay, WA

A Thesis
Presented to
The Faculty of
Western Washington University

In Partial Fulfillment
Of the Requirements for the Degree
Master of Science

by
Brooke A. McIntyre
May 2018

Abstract

Restoring viable, self-sustaining populations of the native Olympia oyster (*Ostrea lurida*) in the Salish Sea is ecologically and socially valuable, because Oysters provide habitat, improve water quality, and are culturally important in the region. Olympia oysters are sessile adults, so they disperse as free-swimming planktonic larvae that actively control their vertical position in the water column with swimming and sinking behaviors, which can affect the currents that carry them and ultimately determine dispersal. Larval dispersal affects population size and connectivity, so understanding dispersal patterns can help managers prioritize habitat restoration efforts to achieve the ultimate goal of establishing a self-sustaining network of Olympia oyster populations throughout the Salish Sea. The purpose of this study was to determine which factors (temperature, chlorophyll-*a*, larval size, current speed, tidal stage) influence the vertical distribution of Olympia oyster larvae in Fidalgo Bay, which is a Washington state priority restoration area for the species. On four consecutive days in July 2017, we collected, counted, and measured the length of Olympia oyster larvae from four depths over the tidal cycle in combination with salinity, temperature, and chlorophyll-*a* measurements. In addition, we deployed an acoustic Doppler current profiler to measure current velocities in the main channel. Mixed effects modelling results indicate that larvae were distributed significantly shallower when current speeds exceeded ~25 cm s^{-1} and deeper when current speeds were less than ~25 cm s^{-1}, but it is unclear whether distribution was due to passive or active larval movement. If larvae were actively controlling their depth, they did not distribute at depth-specific temperature or chlorophyll-*a* conditions, which was likely due to the vertically well-mixed conditions. Larvae were shallower when there was more depth-averaged chlorophyll was in the water column, which might be related to the level of light penetration because Olympia oyster larvae are

phototactic. Larvae did not perform tidally-timed vertical migrations and it remains unclear whether larvae exhibited an ontogenetic vertical migration strategy. Fidalgo Bay does not exhibit a two-way flow or strong vertical shear, so Olympia oyster larval vertical distribution likely has little to no effect on their transport through the main channel of the bay. These results should not be generalized to other restoration areas due to the unique conditions of this location and the possibility of larval behavioral plasticity between distinct populations of Olympia oysters. Results can inform a Fidalgo Bay larval transport model to predict dispersal patterns and prioritize Olympia oyster restoration efforts.

Acknowledgements

First and foremost, my sincere thanks go to my thesis adviser, Dr. Shawn Arellano, for providing exceptional mentorship throughout my thesis research; thank you for always having an open door, for your ongoing support, and for the time you spent to help me become a better scientist. A warm thank you to my committee members Dr. Erika McPhee-Shaw, Dr. Brian Bingham, and Dr. Marco Hatch for the time you spent advising me, for your ideas, your insightful comments, and constructive feedback throughout my thesis work. A specific thank you to Dr. Erika McPhee-Shaw for allowing me to utilize her acoustic Doppler current profiler instrument.

Thank you to the many faculty members at WWU who taught and advised me during this graduate program, especially Dr. Sylvia Yang, Dr. Brady Olson, Dr. Robin Matthews, and Dr. Eric Grossman.

This research would not have been possible without the help from staff and faculty at Shannon Point Marine Center. A big thank you to Captains Nate Schwarck, Gene McKeen, and Jay Dimond for operating research vessels and enabling us to safely collect field data. Thank you specifically to Nate Schwark for advice during field preparations and building a modified bilge pump essential for data collection. Thanks to Dr. Kathy Van Alstyne for lending her Hydrolab equipment.

I am also very grateful for the help I received from many field and lab assistants who generously volunteered their time to collect and process data. Thank you Shay Hengen, Kathryn Williams, Jefferson Emm, Abigail Ernest-Beck, Mia Melamed, Mariah Kollasch, Michael Adamczyk, Aiyi Wu, and Kassey Trahanas. A special thank you to Tyler Tran who was always willing to lend me a hand in the lab, helped me collect data every day of field sampling, and has always provided an endless source of positive energy.

I was able to successfully sort and identify Olympia oyster larvae from my field samples from the generous help from several people. Ryan Crim from the Puget Sound Restoration Fund provided live Olympia oyster larvae and helpful guidance about Olympia oyster spawning. Samish Indian Tribe allowed us to access and collect Olympia oysters from their tidelands. Megan Hintz shared helpful materials and advice on Olympia oyster larval identification. Julie Barber, Sarah Grossman, and Sanoosh Gamblewood with the Swinomish Indian Tribal Community shared information about known local bivalve species and we exchanged helpful advice about identifying larvae throughout the summertime.

Finally, thank you to my family for their relentless support throughout my life and academic career. And a heart-felt thank you to my best friend, Drew Folster. Thank you for your endless patience, support, and optimistic encouragement to help me accomplish my goals.

This work was funded by grants from the National Science Foundation (NSF-OCE-1559940 and NSF-OCE-1538626).

Table of Contents

Abstract……iv

Acknowledgements……vi

List of Tables……viii

List of Figures……ix

Introduction……1

Methods……6

Study location……6

Tidal Currents……6

Larval Abundance and Physical Parameters……7

Larval Identification and Size……8

Data Analysis……9

Results……11

Tidal Currents……11

Physical Conditions……12

Larval Abundance……12

Larval Weighted Mean Depth……13

Discussion……14

Tables……22

Figures……26

Appendix A……35

References……38

List of Tables

Table 1: Linear mixed effects model selection process predicting larval abundance per 100-L sample……22

Table 2: Structure of most parsimonious linear mixed model describing larval abundance per 100-L sample……23

Table 3: Linear mixed effects model selection process predicting larval abundance per 100-L sample……...24

Table 4: Structure of most parsimonious linear mixed model describing larval abundance per 100-L sample……25

List of Figures

Figure 1: Field sampling locations in Fidalgo Bay, WA……..……26

Figure 2: Current velocity (cm s^{-1}) profiles collected by an acoustic Doppler current profiler in the main channel of Fidalgo Bay, WA……...27

Figure 3: Field samples collected on July 11 2017 in Fidalgo Bay, WA…….….28

Figure 4: Field samples collected on July 12, 2017 in Fidalgo Bay, WA…….29

Figure 5: Field samples collected on July 13, 2017 in Fidalgo Bay, WA…….30

Figure 6: Field samples collected on July 14, 2017 in Fidalgo Bay, WA…….31

Figure 7: Larval weighted mean depth over depth-averaged current velocity fit with a GAMM smoother……..32

Figure 8: Larval weighted mean depth versus tidal current speed (cm s^{-1}) and tidal direction….33

Figure 9: Larval weighted mean depth over depth-averaged chlorophyll-*a* (µg L^{-1}) fit with linear mixed effects modeling……..34

Figure A1: Model validation plots for the final linear mixed effects model predicting larval abundance. ……35

Figure A2: Model validation plots for the final linear mixed effects model predicting larval weighted mean depth. ……...36

Figure A3: Generalized additive mixed model results showing the partial effect of current velocity (cm s^{-1}) on larval weighted mean depth.……..37

Introduction

A consortium of stakeholders, including state agencies, tribes, and community members throughout Washington state are working to restore severely reduced Olympia oyster (*Ostrea lurida*) populations because these native bivalves play an important ecological and cultural role in the Salish Sea. Oysters provide ecosystem services like improving water conditions through filtration (zu Ermgassen et al. 2013), forming habitat of shell beds for intertidal organisms, and reducing shoreline erosion (Scyphers et al. 2011). Olympia oysters are also culturally important to native Coast Salish tribes, because they were once an important food source (Steele 1957). However, Olympia oyster populations in the majority of the Pacific Northwest have been classified as poor (reduced by 90%-99%) or functionally extinct (reduced by 99%) due to overharvest in the 1800s and early 1900s (Beck et al. 2011). Recognizing the high ecological and cultural value of the species, the Washington State Department of Fish and Wildlife determined 19 priority restoration sites in 2012 to re-establish Olympia oyster populations in the region (Blake and Bradbury 2012). Collaborative restoration efforts by state, tribal, and non-profit groups have increased the population numbers within a localized area of one priority restoration site—Fidalgo Bay, WA—but work is still underway to grow the population and establish oyster beds throughout the entire bay (Dinnel 2016). The ultimate goal of this restoration is to ensure that Fidalgo Bay has a self-sustaining population that contributes to the larger population network throughout the Salish Sea. To aid localized restoration efforts and determine how connected the Fidalgo Bay population will be with other priority restoration sites, we need a better understanding of how Olympia oysters disperse during their planktonic larval phase.

Larval dispersal, which is the distance larvae travel from the location they are released to the location they settle, can influence the size of the local population, enable colonization of new habitat areas, and determine the degree of connectivity between metapopulations through larval exchange (reviewed by Levin 2006; reviewed by Cowen and Sponaugle 2009). Olympia oysters reproduce and release brooded larvae for just a few months during the summertime; once released into the water column, larvae are transported for one to several weeks by horizontal currents as they grow, develop, and eventually settle in a location with suitable habitat (reviewed by Pritchard et al. 2015). Estimates of population connectivity suggest Olympia oysters have the potential to disperse relatively far distances. For example, Carson (2010) used a trace-elemental fingerprinting technique to estimate that Olympia oyster populations that inhabit bays about fifty miles apart along the southern California coastline are connected. However, current systems in southern California and the Salish Sea are very different, so we need more localized knowledge to understand how larvae will disperse from Fidalgo Bay.

Larval dispersal is affected by both flow and larval behavior (reviewed by Young 1995). Bivalve larvae are transported by horizontal currents, but can actively control their depth through vertical swimming and sinking behaviors, which can determine which horizontal currents carry them (Hidu and Haskin 1978; Shanks and Brink 2005). For example, biophysical transport models that incorporate localized hydrodynamics and larval behavior indicated that eastern oyster larval behaviors can significantly affect transport and dispersal patterns in Chesapeake Bay (e.g. Dekshenieks et al. 1996; e.g. North et al. 2008). Given the potential importance of larval vertical migrations, it is necessary to understand factors that influence the vertical distribution of Olympia oyster larvae to aid their restoration in Fidalgo Bay, but very little is understood about larval swimming behaviors of Olympia oysters.

Bivalve larval behaviors are driven by to both biological and physical factors that enhance development and increase larval survivorship (reviewed by Young 1995). Bivalve larvae alter their vertical distribution behaviors over development; late-stage larvae typically distribute in deeper waters than do early-stage larvae (Carriker 1951; Mann 1988; Baker and Mann 2003) because they tend to be photonegative (Young 1995), geopositive (Young 1995), and sink more quickly than younger larvae (Dekshenieks et al. 1996). Larvae might undergo these ontogenetic behavior shifts to increase dispersal of newly-released larvae away from parental populations and increase retention of late-stage, competent larvae near potential settlement habitat (Dobretsov and Miron 2001; reviewed by Morgan et al. 2014). In addition to internal biological drivers, environmental factors critical to development, like temperature and food availability, also trigger behavioral responses. Temperature directly affects metabolic and growth rates (O'Connor et al. 2007), so larvae behaviorally move away from temperature extremes (Daigle and Metaxas 2011) and may vertically distribute at depths where temperatures are favorable for optimal development. Furthermore, thermoclines affect the depth distribution of bivalve larvae by acting as a barrier to vertical migrations (Tremblay and Sinclair 1988, Gallager et al. 1996, Daigle and Metaxas 2011). Presumably to enhance food availability, bivalve larvae have also been observed to distribute at the chlorophyll-*a* maximum in the field (Raby et al. 1994) and behaviorally respond to food patches in the lab (Metaxas and Young 1998; Sameoto and Metaxas 2008).

Larvae may also exhibit a behavior called selective tidal stream transport where they synchronize their vertical swimming behaviors with the tidal exchange to enhance their export or retention within an estuary (López-Duarte and Tankersley 2009). In estuaries that exhibit a two-layer flow, larvae that occupy deeper water with a net landward current are retained in the

estuary, and larvae that occupy shallower water with a net seaward current are exported to coastal waters (Gibson 2003; Morgan et al. 2014). Selective tidal stream transport is likely a strategy to enhance the probability of larvae settling within areas of suitable habitat and has been observed for several crab species (Welch and Forward 2001; López-Duarte and Tankersley 2009; Morgan et al. 2014). Studies suggest bivalves also exhibit selective tidal stream transport (Carriker 1951; Wood and Hargis 1971; Garrison and Morgan 1999), but it is unclear whether this is true for Olympia oysters. Our preliminary observations in 2014 and 2015 suggest that Olympia oyster larvae do not perform selective tidal stream transport, or tidally-timed vertical migrations, and distribute in surface waters during both ebb and flood in Fidalgo Bay. In contrast, Peteiro and Shanks (2015) found that Olympia oyster larvae do perform tidally-timed vertical migrations by distributing in surface waters during flood tide and bottom waters during ebb tide to enhance retention within the Coos Bay estuary, OR. However, Peteiro and Shanks (2015) only observed this vertical distribution pattern when current speeds were less than 50 cm s^{-1}, which suggests that current speeds greater than 50 cm s^{-1} overwhelm larvae's ability to actively control their depth. The Coos Bay estuary and Fidalgo Bay are unique systems with different conditions, so we should not necessarily expect larvae from these two distinct populations to exhibit the same behaviors. Coos Bay is a relatively large (~ 50 km^2) coastal estuary with a prominent freshwater influence that creates partially-mixed conditions when larvae disperse during the summertime. Fidalgo Bay is a relatively small area (~ 6 km^2) that is connected to a more complex central Salish Sea system, it has very little fresh water influence, and is well-mixed. Moreover, larvae from geographically separate populations may show behavioral plasticity (Manuel et al. 1996; Miller and Morgan 2013), so further investigation is

needed to clarify Olympia oyster larval behavior and vertical distribution patterns in Fidalgo Bay.

The purpose of our study is to gain information that can be used to understand Olympia oyster larval dispersal in Fidalgo Bay to improve restoration activities. Because larval dispersal is a physical and biological process, we investigated the hydrodynamics of tidal currents and factors that influence vertical distribution of Olympia oyster larvae in the bay. Specifically, we characterized the current velocities that move through the prominent main channel in the bay to determine if Fidalgo Bay exhibits vertical shear or a two-layer flow, which would affect transport of larvae distributed at different depths. We also investigated the influence of larval size, which is a proxy for development, temperature, chlorophyll-*a* concentration, current speed, and tides on the depth distribution patterns of Olympia oyster larvae in main channel. Our four hypotheses were the following: (1) larval abundance would be positively related to temperature and chlorophyll-*a*, (2) larvae would not perform tidal vertical migrations based on our preliminary observations in 2014 and 2015 that larvae were more abundant in the surface during ebb and flood tide, (3) larvae would exhibit ontogenetic vertical migrations with more abundant early-stage larvae remaining in surface waters to enhance export and less abundant late-stage larvae remaining in bottom waters to enhance retention, and (4) current speed would significantly influence larval vertical distribution. These results can be used to predict larval dispersal patterns and the population connectivity between the state's priority restoration sites to aid restoration activities and achieve the goal of establishing a self-sustaining network of Olympia oyster populations in the Salish Sea.

Methods

Study location

Fidalgo Bay is adjacent to the city of Anacortes, WA, and two oil refineries in the central Salish Sea. Since 2002 Olympia oyster restoration activities have increased the native oyster population in the bay to an estimated 4.8 million oysters in 2016 (Dinnel 2016). A historic trestle with riprap reinforcement has been converted into a walking path. The trestle channelizes water flow through a prominent main channel of the bay (Figure 1). The bay mostly consists of mudflats and fine sediment habitat that supports large eelgrass beds. The restored oyster beds are adjacent to the main channel along the east side of the bay (Figure 1). Fidalgo Bay is shallow and has no major freshwater input except for runoff from non-point sources, small creeks, and outfalls. It has a semi-diurnal tidal cycle with a mean range of 1.5 meters and is typically unstructured (Murphy et al. 2008), but can develop a thermocline in some areas during the summertime (unpublished data).

Tidal Currents

We programmed and deployed a Nortek 1 MHz Aquadopp acoustic Doppler current profiler (ADCP) fixed to a bottom frame in the main channel of Fidalgo Bay (Figure 1) to record velocity measurements in 0.3 meter vertical bins every 60 seconds. We set out the ADCP in the channel and recorded measurements from 13:00 on July 25, 2017 to 14:00 on July 28, 2017; this timeframe reflected the tides during our week of larvae sampling (see below). The ADCP internally converts raw velocity measures from beam-coordinates into earth-referenced coordinates (north, east, and up) using internal tilt sensor measures. Pitch (-0.03° ± 0.05) and roll (-1.7° ± 0.08) remained small and stable during the deployment. After retrieval, we utilized

Nortek AS software AquaPro version 1.27 to program and retrieve current velocity data from the Aquadopp instrument and MATLAB (Mathworks, Inc.) to process and graph these data for analysis. We performed a principle components analysis (empirical orthogonal function) to determine the depth-averaged principle direction of velocity, which we then utilized to recalculate the coordinate system to match the principle axis of velocity. Using the adjusted coordinate system, we calculated the along-isobath and across-isobath velocity measurements.

Larval Abundance and Physical Parameters

We measured larval abundance, chlorophyll-*a*, temperature, and salinity from four depths at one location by boat each day from July 11 to July 14, 2017 (Figure 1). We chose to sample in July to match the estimated peak reproductive timeframe for Olympia oysters and chose four days with enough tidal exchange to sample during both ebb and flood tide. We collected all samples during daylight hours because Olympia oyster larvae are phototactic (personal observations). Each day, we completed eleven sampling events. During each sampling event, we collected samples from four depths in the water column: surface (0.5 m below surface), bottom (0.5 m above seafloor), and two mid-depth samples, which evenly split the depth between surface and bottom samples. We planned each sampling event to begin at specific times relative to the predicted low tide with the goal of collecting approximately equal numbers of samples during ebb and flood tide. It took 15-20 minutes to collect all four samples during each sampling event. By the end of the four consecutive sampling days, we had performed 44 sampling events and collected a total of 176 individual samples.

To collect each larval sample, we used a modified bilge pump to filter 100 liters of water from our targeted depths through a 102 µm mesh plankton net to ensure retention of Olympia

oyster larvae, which are released from brooding with a ~180µm length shell (reviewed by Pritchard et al. 2015). Each sample was stored on ice while in the field and then preserved in 70% ethanol. At the end of filtering each 100-L sample, we collected 60 ml of bulk seawater from the pump for measurement of chlorophyll-*a*. We filtered the 60 ml of seawater through a glass microfiber filter (Whatman™ GF/F). The foil-wrapped filters were held on ice in the field and then stored them at -80°C for later extraction. We measured chlorophyll-*a* concentration from each filtered sample by extracting the chlorophyll-*a* pigment using 90% acetone for 24 hours and reading fluorescence of each sample with a Turner Trilogy Fluorometer. We programmed a Hach Environmental Company HydroLab DS5 water quality multiprobe instrument to collect temperature and salinity measurements at the same times and depths as our pump sampling. A Hach Hydras 3 Pocket instrument enabled us to calibrate, program, and retrieve data from the HydroLab. We used along-isobaths data from the ADCP to determine a current velocity for each event and sample based on corresponding time and depth.

Larval Identification and Size

We used an Olympus Optical Company SZ-ST stereoscope fit with polarized lens filters to hand sort Olympia oyster larvae from each sample. Olympia oyster larvae were identified from the other bivalves in our sample using several methods. First, we narrowed down all the potential local species of bivalve larvae that might be in our samples based on reproductive season (Loosanoff et al. 1966, personal communication Julie Barber). We then distinguished Olympia oyster larvae from these other species by comparing morphological features relative to size based on identification keys (Loosanoff et al. 1966, Shanks 2001) and reference Olympia oyster larvae that we reared in the laboratory. Reference larvae were fixed and photographed under an Olympus CH-2 microscope to aid identification. We measured shell lengths perpendicular to the

hinge of each larva digitally using a stereomicroscope equipped with a camera and ImageJ software (Leica MC170 HD and Leica Application Suite, Leica, Wetzlar, Germany). Larvae were divided into three distinct size classes: 180-210 μm were newly-released larvae, 211-260 μm were developing larvae, and >260 μm were late-stage larvae close to settlement. We chose these size classes according to reference materials (Loosanoff et al. 1966, Shanks 2001) and personal observations of how larval size increases during development of lab reared Olympia oyster larvae from the Fidalgo Bay population.

Data Analysis

To investigate relationships between measured parameters and vertical distribution of larvae, we fit mixed effects models. Mixed effects models account for violations of independence and give structure to the residual error term by allowing the modeler to include random effects that account for unavoidable sources of variability and non-independence within the sampling design. These models also account for violations of homogeneity by enabling the modeler to manipulate the variance structure to improve residual structure (Zuur et al. 2009; Winter 2014). Each model included all four days of sampling data.

We represented the vertical distribution of larvae in two distinct ways to use as response variables in separate models: (1) larval abundance per sample and (2) larval weighted mean depth (WMD) normalized to water column height per sampling event. Larval abundance per sample is the total number of Olympia oyster larvae per 100 L depth-specific sample. Larval WMD gives a single value to represent the vertical distribution of larvae for statistical comparison. The following equation is used to calculate the normalized larval weighted mean depth (WMD).

$$WMD = \left(\frac{\sum A_i z_i}{\sum A_i}\right)(H^{-1})$$

A_i is the abundance of larvae in the ith layer

z_i is the mid-depth of the ith layer

H is the water column height (m) at the time of sampling

Each WMD measurement was a ratio from 0-1, with low values representing shallower larval WMD and high values representing deeper WMD.

For each model, we started with a model containing all predictor variables of interest and then determined the most parsimonious fit by comparing models with log likelihood tests and Akaike information criterion (AIC) to inform the model selection process. We then calculated the conditional and marginal R^2 values for each final model, which indicate variance explained by the entire model and by the fixed factors alone, respectively ("MuMIn" package in R 3.3.1, R Core Team 2016; Nakagawa and Schielzeth 2013; Bartoń 2017). We validated the fit of each final model by visually inspecting residual plots to verify homogeneity and QQ-plots to verify normality. Additionally, we inspected data for temporal autocorrelation structures using autocorrelation function plots.

We fit a linear mixed effect model (LME) to investigate the fixed effects of depth (m), current velocity (m s^{-1}), temperature (°C), and chlorophyll-*a* (µg L^{-1}) on the abundance of larvae per 100-L sample ("nlme" package in R 3.3.1, R Core Team 2016; Pinheiro et al. 2017). We included a random intercept of 'sampling event' nested within 'sampling day' to account for this inherent non-independence of our sampling design. In addition, we built the model to allow for unique variance structures by water column height to correct for an observed violation of variance homogeneity.

To investigate predictors of larval WMD, we fit a generalized additive mixed model (GAMM) and a linear mixed effect model (LME). Preliminary plots suggested a non-linear relationship between larval WMD and depth-averaged current velocity, so we fit a GAMM with a thin plate regression spline for the depth-averaged velocity parameter to investigate the significance of this non-linear relationship ("mgcv" package of R 3.3.1, R Core Team 2016; Wood 2011). We then fit an LME to investigate the fixed effects of depth-averaged absolute current speed (cm s^{-1}), current direction (ebb or flood), depth-averaged chlorophyll-*a* (µg L^{-1}), and proportion of newly-released larvae (180-210 µm) on larval WMD ("nlme" package of R 3.3.1, R Core Team 2016; Pinheiro et al. 2017). We included a random intercept for 'sampling event' to account for this violation of independence in our sampling design. A log likelihood ratio test using REML estimation indicated that including sampling day as an additional part of the random component did not improve the model, so we removed this term to reduce model complexity. We performed a simple contrast from the full LME model to compare larval WMD on ebb versus flood tide after ensuring equal variance using a Levene's test ("gmodels" and "car" packages of R 3.3.2, R Core Team 2016; Fox and Weisberg 2011; Warnes et al. 2015). Lastly, we compared the WMD of the three size classes of larvae (180-210µm, 210-259µm, and >260µm) with a 1-way ANOVA after applying a Levene's test to verify that the equal variance assumption was satisfied.

Results

Tidal Currents

The dominant tidal currents flowed along Fidalgo Bay's main channel with negligible cross channel flow (Figure 2). Along-channel currents flowed at velocities below |50| cm s^{-1} during periods of low tidal exchanges, which corresponds with the timeframe during each of our four

larval sampling days. Fidalgo Bay did not exhibit a two-way current flow. Also, there was little to no vertical shear through the water column, but when the currents slow near slack tide the water along the seafloor appeared to slow and flood a bit sooner than waters near the surface. Vertical velocities were slightly positive (3.8 ± 3.5 cm s^{-1}) and showed no evident pattern of upward and downward water movement in relation to certain periods of the tidal cycle throughout the deployment (Figure 2).

Physical Conditions

During each day of larval sampling by boat the water column was shallow (2.5 – 5 m) and conditions were sunny with light winds (<10 mph). There was little to no salinity structure in the water column (28.91 ± 0.25) and vertical profiles were consistently well-mixed. Temperatures ranged from about 12 to 19°C (16.6 ± 1.3 °C) with little stratification and thermal profiles changed in a consistent pattern over each day. The water column was generally well-mixed and steadily increased in temperature during ebb tide, peaked in temperature near slack tide, and then became stratified during flood tide (Figure 3). The maximum change in temperature from surface to bottom was 1.1 °C during ebb tide and 4.1 °C for a few sampling events during flood tide. Chlorophyll-*a* ranged from 4.4 to 38.6 µg L^{-1} (19.1 ± 8.1 µg L^{-1}), but there were no evident chlorophyll-*a* maxima per sampling event or pattern in abundance or distribution of chlorophyll-*a* over each sampling day (Figure 3 - 6). Secchi depths remained between 0.75 and 1 m throughout one full day of sampling.

Larval Abundance

Depth distribution of larvae varied over the tidal cycle each day, but did not appear to be related to depth-specific current velocity, temperature, or chlorophyll conditions (Figures 3- 6). These

observations were supported by the linear mixed effects model, which indicated that depth was the only factor that significantly affected larvae abundance per sample (Tables 1 and 2, Figure A1).

Larval Weighted Mean Depth

Larval vertical distribution patterns throughout the tidal cycle were similar on all four of our sampling days. Depth profile plots reveal that larvae were shallower during relatively fast, ebb tide currents, deepened as the currents slowed around slack tide, and were shallower when current velocities increased on flood tide (Figure 3 - 6). Supporting this pattern, a generalized additive mixed model indicated that larval weighted mean depth (WMD) and depth-averaged current velocity had a significant non-linear relationship (GAMM, $F_{edf\ of\ 4} = 11.7$, $p << 0.001$; Figure 7, Figure A3). More specifically, absolute depth-averaged current speed, not current direction (ebb or flood), significantly affected larval WMD (LME, Table 3, Table 4, Figure 8). Larval WMD was shallower during ebb and flood tides when current speeds were greater than ~25 cm s^{-1} and deeper when current speeds were less than ~25 cm s^{-1}, which occurred around slack tide. In addition, larval WMD was significantly shallower when more depth-averaged chlorophyll-*a* (µg L^{-1}) was in the water column (LME, Table 3, Table 4, Figure 9).

Every size class of larvae exhibited the same WMD pattern in relation to tidal currents (Figure 7), and this observation is confirmed by the LME model selection process indicating that proportion of newly released larvae (180-210µm) does not significantly affect larval WMD (Table 3, Table 4, Figure A2). Additionally, a 1-way ANOVA indicated no significant variation in the WMD among the three pre-selected size classes of larvae ($F_{2,129} = 1.81$, $p = 0.17$). The η^2 was 0.03, indicating that size-class to size-class differences accounted for just 3% of the total

variability in larval WMD. Out of the total larvae sampled (n=10,124), 48% were 180-210µm, 43% were 210-260µm, and 7% were >260µm.

Discussion

Olympia oyster larvae in Fidalgo Bay were distributed significantly shallower when current speeds exceeded ~25 cm s^{-1} during both ebb and flood tide and deeper when current speeds decreased below ~25 cm s^{-1} during slack tide (Figure 7, Figure 8), but it is unclear whether distribution was due to passive or active larval movement. Vertical velocity profiles did not indicate a downward movement of water during slack periods of the low tidal exchanges sampled (Figure 2), so the vertical current velocities alone do not explain differences in larval WMD between periods of faster and slower horizontal currents (Figure 7). A study using a biophysical model in shallow (< 5 m), well-mixed areas of Delaware Bay, similar to conditions in Fidalgo Bay, predicted that oyster larvae (*Crassostrea virginica*) and passive particles exhibit similar dispersal patterns (Narváez et al. 2012). However, several other studies suggest that bivalve larvae do not behave like passive particles (e.g. Carriker 1951; Wood and Hargis 1971; North et al. 2008) and are capable of active depth distribution in horizontal current speeds as high as 50 cm s^{-1} (Mann et al.1988, Kim et al. 2010, Peteiro and Shanks 2015).

Oyster larvae behaviorally respond to hydrographic conditions, which might have enabled Olympia oyster larvae in Fidalgo Bay to influence their vertical distribution over our sampling period. In flume and grid-stirred flow tank experiments, eyed eastern oyster larvae (*Crassostrea virginica*) actively respond to hydrographic cues related to turbulence by swimming upward faster or by rapidly diving (Finelli and Wethey 2003; Fuchs et al. 2013; Fuchs et al. 2015; Wheeler et al. 2015). Finelli and Wethey (2003) estimated that when larvae dive at 0.8 cm s^{-1}, which is the maximum downward velocity we measured for late-stage Olympia oyster

larvae in the lab, they exert enough propulsive force to potentially control their depth in horizontal current speeds up to 17-52 cm s^{-1}. This estimation was based on two assumptions: (1) that larvae can control their vertical position when Rouse numbers, which are ratios of sinking velocity over shear velocity, are greater than 0.75 (Gross et al. 1992), and (2) that shear velocity is 0.05 to 0.15 times freestream velocity over smooth bottoms (Finelli and Wethey 2003). Recognizing that Fidalgo Bay does not have a smooth bottom, we can still use the same logic as Finelli and Wethey (2003) to hypothesize that Olympia oyster larvae in Fidalgo Bay could have been actively responding to hydrographic conditions and regulating their depth because current speeds remained below 50 cm s^{-1} over the duration of our larval sampling period. This hypothesis is further supported by Peteiro and Shanks (2015) who observed Olympia oyster larvae in Coos Bay estuary distribute significantly deeper during ebb than flood tides when currents speeds were less than 50 cm s^{-1}, but became evenly distributed throughout the water column when current speeds increased above 50 cm s^{-1}.

If observed larval distribution patterns were not simply passive and larvae were actively controlling their depth, our results suggest some larval behavioral strategies that may explain our observation that larvae distributed in surface waters during both ebb and flood tide, but deeper during slack tide. First, larvae might have behaviorally responded to hydrographic cues by swimming upward faster during higher current speeds. Eyed eastern oyster larvae increase upward swimming speeds and occasionally actively dive when turbulence increases in flume and grid-stirred flow tank experiments (Wheeler et al. 2013; Fuchs et al. 2015). Olympia oyster larvae might have been responding like these species if turbulence increases with current speed in Fidalgo Bay. However, a more thorough exploration of this hypothesis would benefit from

future studies defining the turbulence conditions in Fidalgo Bay and investigating behavioral responses specifically of Olympia oyster larvae to turbulence.

Larval abundance was not positively related to depth-specific temperature and chlorophyll-*a* as hypothesized, indicating that larvae did not distribute at depths with warmer water or more abundant phytoplankton. We likely observed these results because our sampling location in the main channel during the low tidal exchange was relatively shallow (2.5-5.5 meters), thermally well-mixed, and likely not food-limited based on measurements of chlorophyll-*a* at every depth. Bivalve larvae avoid temperature extremes (Daigle and Metaxas 2011; Civelek et al. 2013) and might distribute in relation to thermoclines (Manuel et al. 1996; Lloyd et al. 2012) to inhabit favorable conditions for development (Young 1995). Bivalve larvae also respond to food cues in the lab (Sameoto and Metaxas 2008) and aggregate at chlorophyll maxima in deep, food-limited areas (Raby et al. 1994). Our sampling location remained within favorable temperature ranges and was typically well mixed, so temperature did not drive the pattern we observed in larval distributions. We also measured chlorophyll-*a* at all depths with no clear chlorophyll maxima, so it is not surprising larvae did not distribute in relation to depth-specific chlorophyll-*a*. Temperature and chlorophyll-*a* would likely be more influential predictors of larval abundance at times and locations in Fidalgo Bay when the water is deeper with strong thermoclines, which can occasionally be observed in Fidalgo Bay (personal observations).

Surprisingly, while larvae did not seem to distribute in response to depth-specific chlorophyll-*a* conditions, they were distributed significantly shallower when there was more average chlorophyll in the water column (Figure 9). These results were significant even taking into account the time of day and water column height (Table 4). Although the relationship is

significant, depth-averaged chlorophyll-*a* only accounted for an estimated ~13% of variance in predicting larval WMD (Table 4), suggesting this is probably not a strong driver of vertical distribution of Olympia oyster larvae. Nonetheless, this observation hints at a possible relationship between larval depth distribution and light conditions because abundance of phytoplankton affects the depth of light penetration. Like other larval bivalves (Bayne 1964; Barile et al. 1994), Olympia oyster larvae are highly phototactic (unpublished observations), so when high abundances of phytoplankton block light from penetrating as deeply into the water, Olympia oyster larvae might distribute shallower. While equipment failure prevented us from measuring light at our sampling depths, we measured secchi depths between just 0.75 and 1 meter deep during an entire day of sampling, which suggests that even in shallow waters (2.5-5.5 m) in Fidalgo Bay, light conditions might be an important predictor of larval distribution. However, if larvae were behaviorally swimming upward due to a photopositive response, we would expect them to remain in surface waters throughout the tidal cycle, which we did not observe. In fact, larvae were distributed deeper during slack tide when they would likely have the most control over their vertical position due to slower current speeds. Based on these observations, photopositive behavior does not fully explain our observed larval distributions. While light might play a partial role in larval vertical distributions, one or more other factors might also be at play.

Although mixed modelling indicated that larval size was not a significant predictor of larval weighted mean depth, it remains unclear whether Olympia oyster larvae in Fidalgo Bay exhibit an ontogenetic migration strategy. On one hand, ontogenetic shifts appear to be species-specific (Baker and Mann 2003), so Olympia oyster larvae might not exhibit the ontogenetic vertical migrations seen with other oyster species in which late-stage larvae distribute deeper than early-

stage larvae (Andrews 1983; Mann 1988). On the other hand, our sampling design might have failed to detect an ontogenetic vertical migration behavior in Olympia oyster larvae in Fidalgo Bay. Only about 7% of the total larvae we sampled were greater than 260μm in length, which is the size Olympia oyster larvae begin to develop a foot and become competent to settle (Loosanoff et al. 1966; personal observations). While we expected to collect fewer late-stage larvae due to mortality and possible export from the bay, 7% is still relatively low compared to the high levels of observed recruitment in the Fidalgo Bay population (Dinnel et al. 2009). The low representation of large, late-stage larvae suggests that these individuals might have been remaining closer to the sediment interface than we were sampling. The deepest sample we collected in our sampling design was always 0.5 m above the seafloor, so we might have missed the majority of late-stage larvae if they were aggregating deeper very close to the seafloor. In the lab, other species of large, competent oyster larvae remain within just a few body lengths from the seafloor (Jonsson et al. 1991; Finelli and Wethey, 2003). If more late-stage Olympia oyster larvae were, indeed, nearer the seafloor than we sampled, the high representation of early- and developing-stage larvae in surface waters during both ebb and flood tide provide evidence of an ontogenetic vertical migration strategy.

Although we were unable to confidently distinguish evidence for or against ontogenetic vertical migrations, Olympia oyster larvae in Fidalgo Bay did not perform tidal vertical migrations as they did in Coos Bay (Peteiro and Shanks 2015). Similar to our preliminary observations in 2014 and 2015, we found more larvae in surface waters during ebb and flood tide in Fidalgo Bay. In contrast, Peteiro and Shanks (2015) observed more larvae in surface waters during flood tide and more larvae in bottom waters during ebb tide. These contrasting results might indicate behavioral plasticity between these two geographically distinct populations to

optimize larval survivorship in differing conditions. Larvae in Coos Bay must be retained within the estuary to avoid wastage from being swept out to the open coast (Peteiro and Shanks 2015), but this is not the case for larvae released from Salish Sea populations. Historic populations were spread throughout the Salish Sea region (Blake and Bradbury 2012) and larvae had opportunities to encounter habitat even if transported far from their natal population. Therefore, oysters in the Salish Sea might have adapted different behavioral strategies than oysters in outer coastal estuaries, such as the Coos Bay estuary. Instead, larvae in Fidalgo Bay may have been lacking an environmental cue like salinity to trigger tidally-timed vertical migration given Fidalgo Bay's well-mixed and low-inflow conditions. Salinity gradients cue tidal migrations for eastern oyster and crustacean larvae by triggering upward swimming in increased salinity and sinking in lower salinity (Hidu and Haskin 1978; Dekshenieks et al. 1996; Welch and Forward 2001; Miller and Morgan 2013). Crustacean species known to perform tidal migrations in stratified coastal waters did not perform these behaviors in low-inflow, well-mixed estuaries, presumably because the salinity signal was too weak to trigger behavior or vertical mixing overwhelmed active depth regulation (Miller and Morgan 2013; Morgan et al. 2014). In the Salish Sea, we might expect Olympia oyster larvae to exhibit tidal vertical migrations in habitats with higher freshwater influence than Fidalgo Bay.

The influence of larval behavior is system-dependent based on oceanographic current regimes. In some systems biophysical transport models that incorporate active particles indicate behavior can significantly influence oyster larval transport and dispersal patterns (eg. Dekshenieks et al. 1996; North et al. 2008), but models used in other systems suggest behavior has little to no effect on transport (Kim et al. 2010; Narváez et al. 2012; Thomas et al. 2014). Although our results indicate that newly-released and developing Olympia oyster larvae in the

main channel of Fidalgo Bay distribute within surface waters (~0.5-1.5m) during strong tidal currents on both ebb and flood tide, these behaviors may not affect dispersal in Fidalgo Bay. Larvae that occupy surface waters will have enhanced export in estuaries that exhibit a two-layer flow (Dyer 1997; reviewed by Morgan et al. 2014), but our data indicate that the main channel in Fidalgo Bay does not exhibit two-layer flow or strong vertical shear. Given the flow of currents in Fidalgo Bay, Olympia oyster larvae behavior and vertical distribution likely has little to no effect on their transport through the main channel of the bay.

Although larval vertical distribution might not be a strong driver of transport in Fidalgo Bay, it could be an important driver of transport in other Salish Sea locations. Fidalgo Bay has very little freshwater input and highly channelized tidal currents, and, thus, is a fairly unique environment in the Salish Sea. Fidalgo Bay's conditions might be representative of potential larval settlement areas and habitat in the San Juan Islands that also have little freshwater influence, but are likely very different from the majority of other state priority restoration sites that have stronger freshwater influence. In addition to altered hydrodynamics at these locations, the freshwater influence might provide a salinity cue that could change larvae behavioral patterns and larvae from geographically separate populations may exhibit behavioral plasticity (Miller and Morgan 2013). Therefore, these data should not be generalized to how larvae will vertically distribute in locations throughout the Salish Sea. These results highlight the importance of understanding the local physical and hydrodynamic conditions of an area and underscore the importance of gaining localized knowledge about larval vertical distributions to make confident predictions about larval transport and dispersal patterns.

Results from this study can inform both the hydrodynamic and biologic components of a Fidalgo Bay larval transport model to predict larval dispersal patterns. Understanding Olympia

oyster larval transport and dispersal from Fidalgo Bay and other restoration sites can help managers predict source and sink locations of larvae and prioritize habitat restoration efforts to achieve the ultimate goal of establishing a self-sustaining network of Olympia oyster populations throughout the Salish Sea.

Table 1. Model selection process using log-likelihood ratio tests and comparing AIC and BIC values to determine which fixed effects predict larval abundance per sample and includes data from all sampling days. Fixed effects include depth of sample (Depth), current velocity (CurrentVelocity), temperature at the sampling depth (Temp), and average chlorophyll-*a* at the sampling depth (Chl-*a*). Each log-likelihood ratio test statistically compares the goodness of fit of the full model, which contains all fixed effects, against the goodness-of-fit of a reduced model, which has one fixed effect removed. All models have the same random effects, so they are considered to be nested models. The p-value is the likelihood of calculating the log-likelihood ratio test statistic (L.Ratio) indicated in the table if the null hypothesis, which is that the full model has a better fit than the reduced model, is true. We determined the statistical significance of each fixed effect by removing each one from the full model in turn.

Model	Model in comparison	df	AIC	BIC	logLik Ratio	L.Ratio	p
1) Abundance ~ Depth + CurrentVelocity + Temp + Chl-*a*	--	21	1734.13	1800.71	-846.07		
2) Abundance ~ Depth + CurrentVelocity + Temp	1	20	1732.14	1795.55	-846.07	0.0073	0.93
3) Abundance ~ Depth + CurrentVelocity + Chl-*a*	1	20	1732.24	1795.65	-846.12	0.1087	0.74
4) Abundance ~ Depth + Temp + Chl-*a*	1	20	1732.13	1795.54	-846.07	0.0020	0.96
5) Abundance ~ CurrentVelocity + Temp + Chl-*a*	1	20	1768.13	1831.54	-864.07	35.998	<0.001
6) Abundance ~ Depth	1	18	1728.66	1785.73	-846.33	0.5284	0.91

Table 2. Structure of most parsimonious linear mixed model describing larval abundance per sample. Final model factors chosen based on AIC value comparisons and log likelihood ratio tests.

Fixed Effects

Parameter (Final Model)	Value	SE	DF	t	p
Intercept	68.97	5.00	131	13.79	<0.001
Depth (m)	-11.03	1.31	131	-8.40	<0.001

Parameter (Removed during model selection)

Temperature (°C)
Chlorophyll-*a* (μg L^{-1})
Current Velocity (m s^{-1})

Random Effects

Random intercept given to each 'sampling event' nested within each 'sampling day'.

Unique variance structures allowed for varying water column height.

Marginal R^2 (variance explained by fixed effects): 24.8%
Conditional R^2 (variance explained by entire model): 50.7%

Table 3. Model selection process using log likelihood ratio tests and comparing AIC and BIC values to determine which fixed effects explain significant amount of variance for larval WMD and includes data from all sampling days. These fixed effects include average chlorophyll-*a* (Chl-*a*), depth averaged absolute current speed (CurrentSpeed), current direction (Tide), and proportion of newly released larvae (PropNew). Each log-likelihood ratio test statistically compares the goodness of fit of the full model, which contains all fixed effects, against the goodness-of-fit of a reduced model, which has one fixed effect removed. All models have the same random effects, so they are considered to be nested models. The p-value is the likelihood of calculating the log-likelihood ratio test statistic (L.Ratio) indicated in the table if the null hypothesis, which is that the full model has a better fit than the reduced model, is true. We determined the statistical significance of each fixed effect by removing each one from the full model in turn.

Model	Model in comparison	df	AIC	BIC	LogLik	L.Ratio	p
1) WMD ~ Chl-*a* + CurrentSpeed + Tide + PropNew	--	6	-111.51	-99.02	62.75		
2) WMD ~ Chl-*a* + CurrentSpeed + Tide	1	5	-113.19	-102.48	62.59	0.3228	0.57
3) WMD ~ Chl-*a* + CurrentSpeed + PropNew	1	5	-112.88	-102.18	62.44	0.6283	0.42
4) WMD ~ Chl-*a* + Tide + PropNew	1	5	-98.96	-88.25	55.47	14.55	<<0.001
5) WMD ~ CurrentSpeed + Tide + PropNew	1	5	-102.97	-92.27	57.48	10.53	0.0012
6) WMD ~ Chl-*a* + CurrentSpeed	1	5	-114.54	-105.61	62.27	0.6503	0.42
7) WMD ~ Chl-*a*	6	4	-102.63	-95.5	55.32	13.90	<<0.001
8) WMD ~ CurrentSpeed	6	4	-103.89	-96.75	55.94	12.64	<<0.001

Table 4. Structure of most parsimonious linear mixed effects model describing larval weighted mean depth. Final model factors chosen based on AIC value comparisons and log likelihood ratio tests.

Fixed Effects

Parameter	Estimate	SE	T	p	Marginal R^2
Intercept	0.62	0.028	21.8	<<0.001	
Current Speed (m s^{-1})	-0.38	0.08	-4.87	<<0.001	0.442
Depth-averaged Chlorophyll-*a* (µg L^{-1})	-0.004	0.001	-3.80	<<0.001	0.125

Parameter (Removed during model selection)
Proportion Newly Released
Current Direction/Tide

Random Effects

Random intercept given for each sampling event.

Marginal R^2 (variance explained by fixed effects): 55.9%
Conditional R^2 (variance explained by fixed and random effects): 63.3%

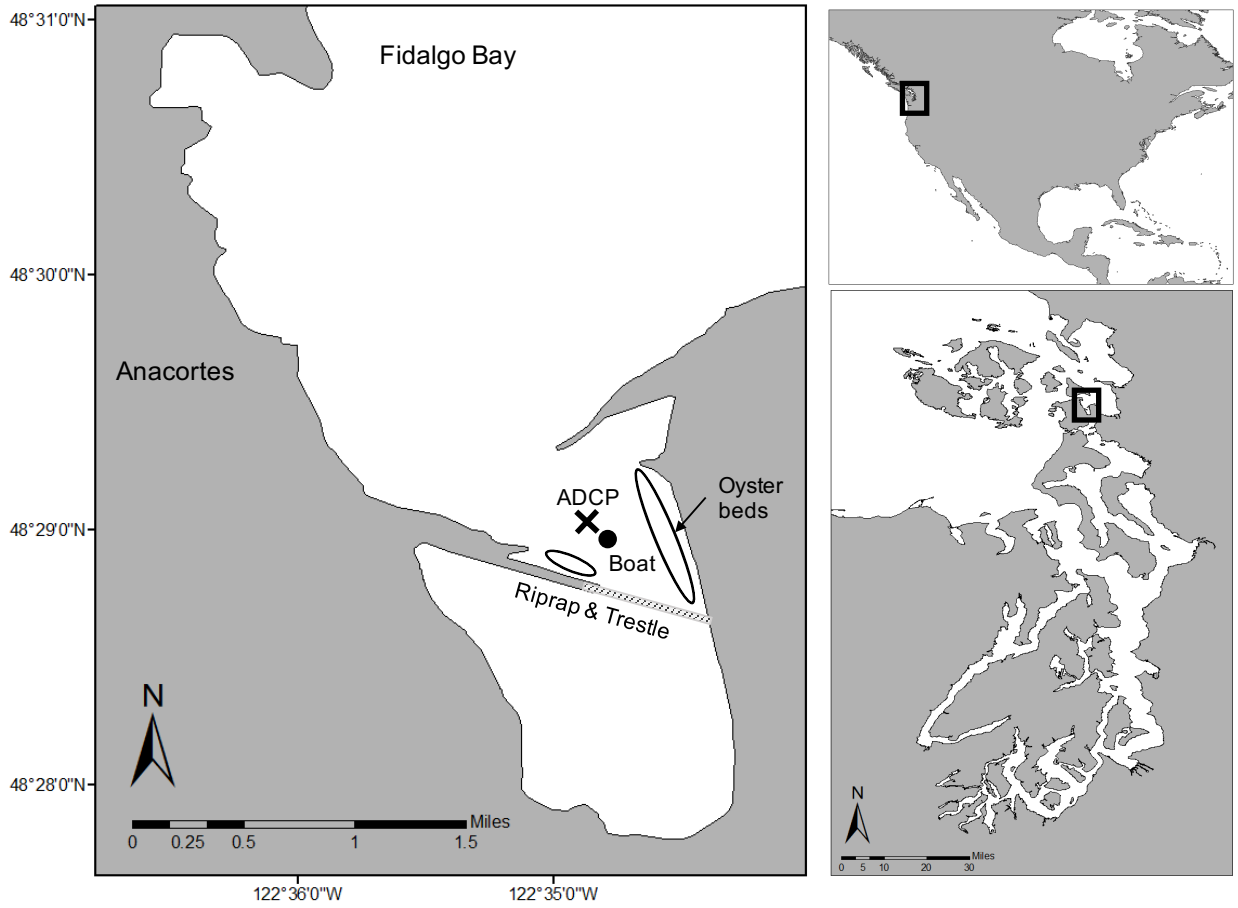

Figure 1. Fidalgo Bay, adjacent to Anacortes, WA, is a priority restoration site for the Olympia oyster and our field sampling location. A black dot indicates the location we collected samples by boat (48.4823, -122.58) July 11th through July 14th, 2017. A black "x" indicates the location we deployed the acoustic Doppler current profiler to measure current velocity profiles (48.4828, -122.5811) July 25th through July 28th, 2017. Olympia oyster beds are circled.

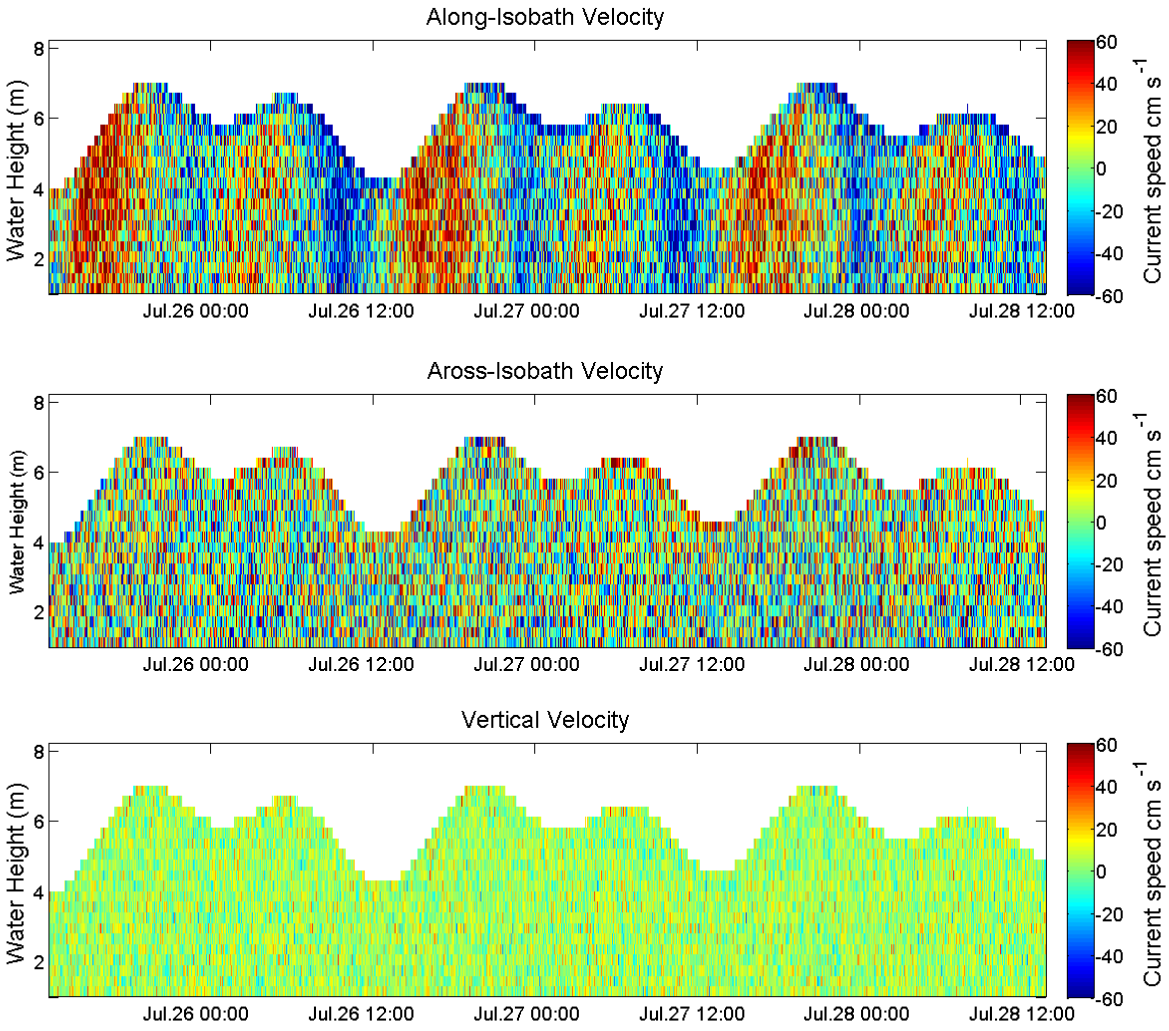

Figure 2. Along-isobath, across-isobath, and vertical current velocities (cm s^{-1}) over the height of the water column (m) collected by an Aquadopp 1 mHz acoustic Doppler current profiler every 60 seconds in 0.3 m depth increments from July 25th at 13:00 through July 28th at 14:45 in the main channel of Fidalgo Bay. Along-isobath values represent water moving with the main channel and across-isobath represents water moving across the main channel. The color scale bar on the right-hand side of each plot displays the current speed (cm s^{-1}). For the along- and across-isobath plots positive current speed values correspond with water rising on a flood tide and negative current speed values correspond with water leaving on an ebb tide. For the vertical velocity plot positive values correspond with upward movement and negative values correspond with downward water movement.

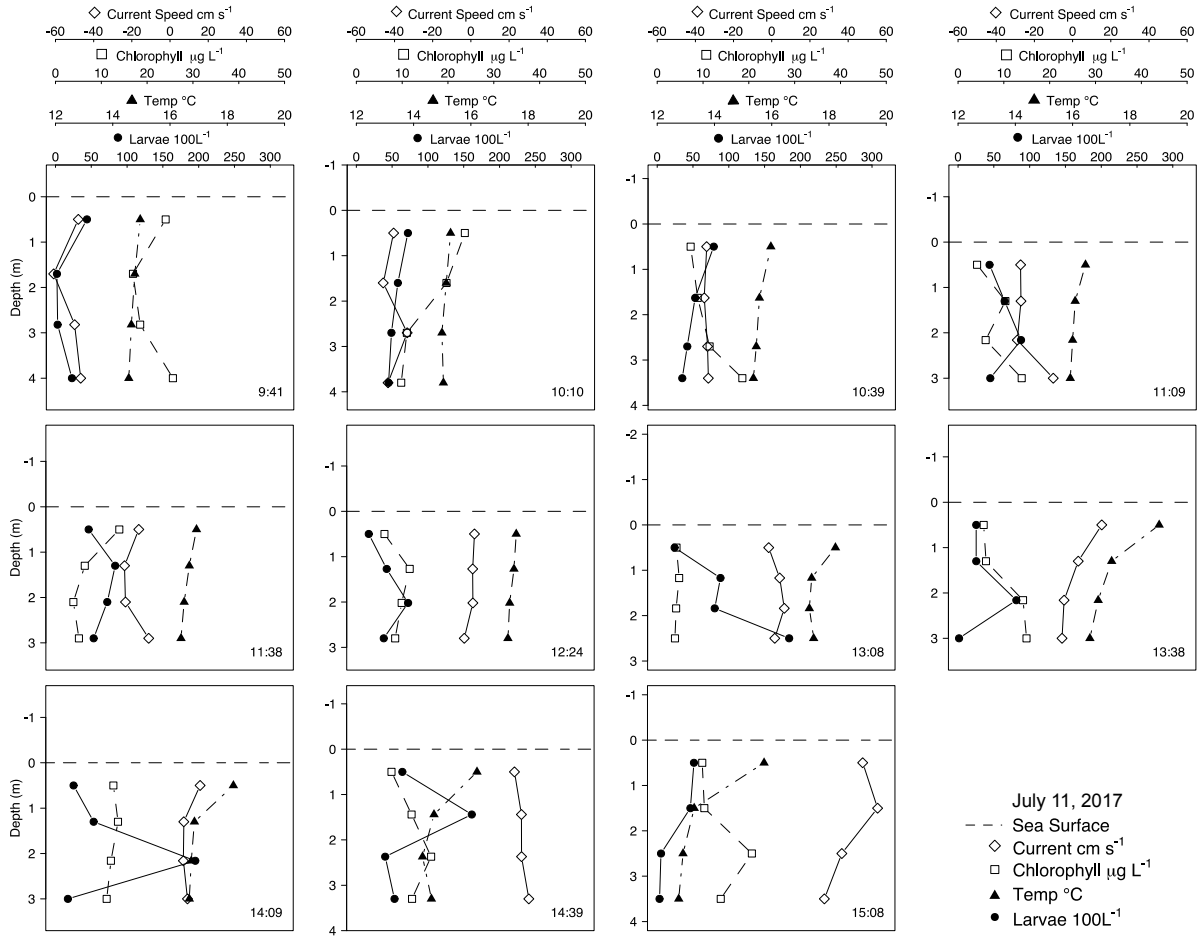

Figure 3. Field samples collected on July 11, 2017 in Fidalgo Bay. Each plot shows one sampling event, which includes samples collected at four depths beginning at the time listed in the bottom right corner. Black circles represent the number of larvae collected in 100L of pumped water, gray triangles show the water temperature (°C), white squares represent the chlorophyll-*a* (µg L^{-1}), and white diamonds represent current velocity (cm s^{-1}). Negative values of current velocity indicate water moving out of the bay (ebb tide) and positive values indicate water moving into the bay (flood tide). The horizontal dotted line represents the sea surface, which adjusts accordingly so the bottom of each plot represents the seafloor.

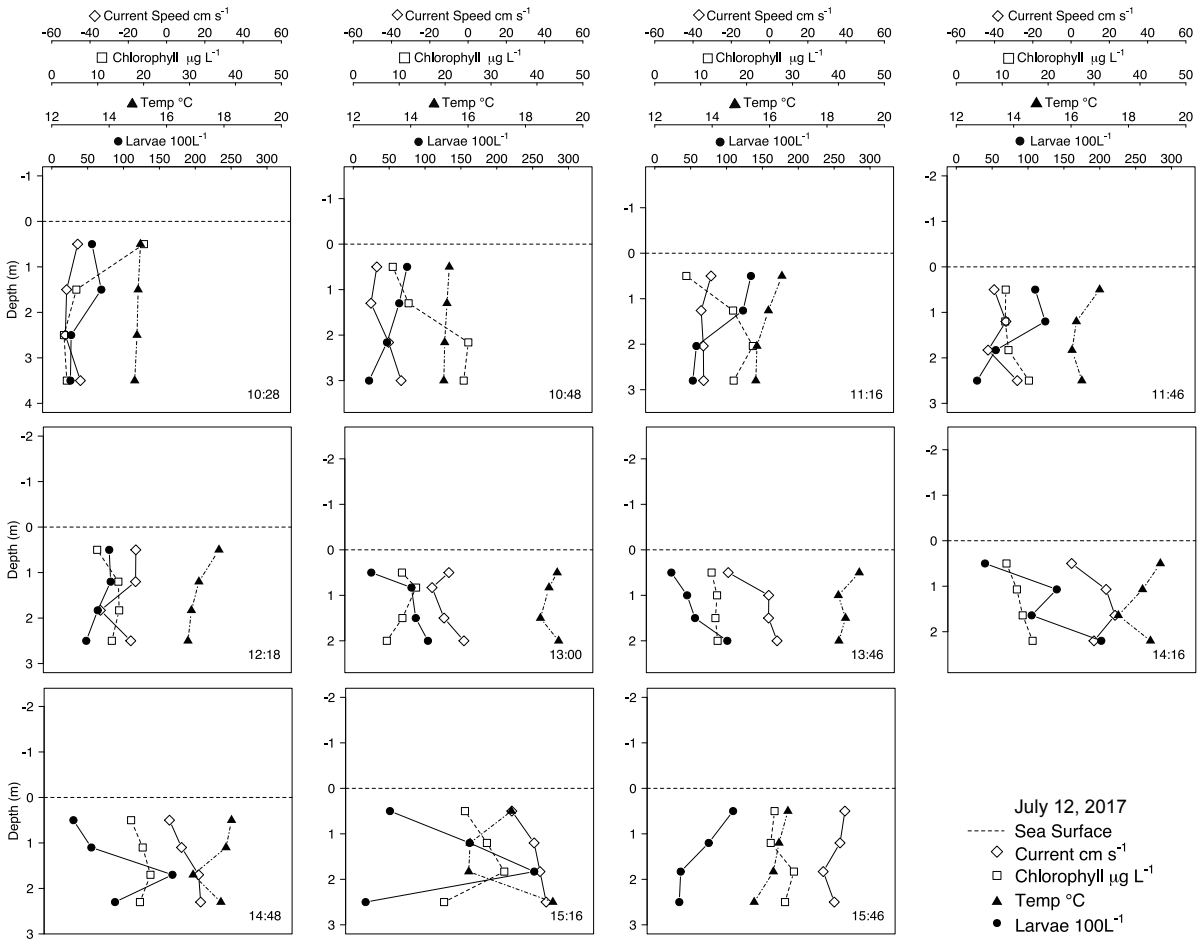

Figure 4. Field samples collected on July 12, 2017 in Fidalgo Bay. Each plot shows one sampling event, which includes samples collected at four depths beginning at the time listed in the bottom right corner. Black circles represent the number of larvae collected in 100L of pumped water, gray triangles show the water temperature (°C), white squares represent the chlorophyll-*a* (µg L^{-1}), and white diamonds represent current velocity (cm s^{-1}). Negative values of current velocity indicate water moving out of the bay (ebb tide) and positive values indicate water moving into the bay (flood tide). The horizontal dotted line represents the sea surface, which adjusts accordingly so the bottom of each plot represents the seafloor.

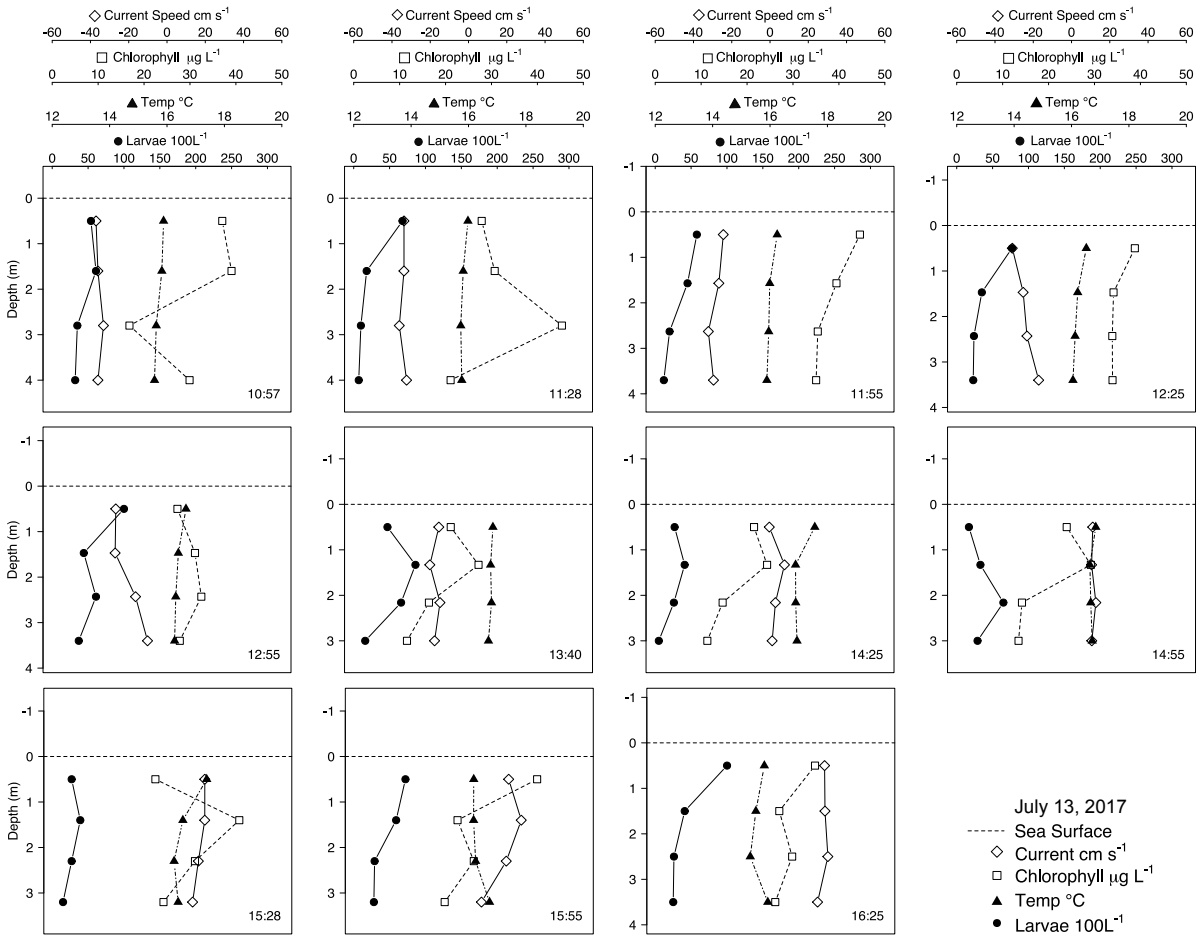

Figure 5. Field samples collected on July 13, 2017 in Fidalgo Bay. Each plot shows one sampling event, which includes samples collected at four depths beginning at the time listed in the bottom right corner. Black circles represent the number of larvae collected in 100L of pumped water, gray triangles show the water temperature (°C), white squares represent the chlorophyll-*a* (µg L^{-1}), and white diamonds represent current velocity (cm s^{-1}). Negative values of current velocity indicate water moving out of the bay (ebb tide) and positive values indicate water moving into the bay (flood tide). The horizontal dotted line represents the sea surface, which adjusts accordingly so the bottom of each plot represents the seafloor.

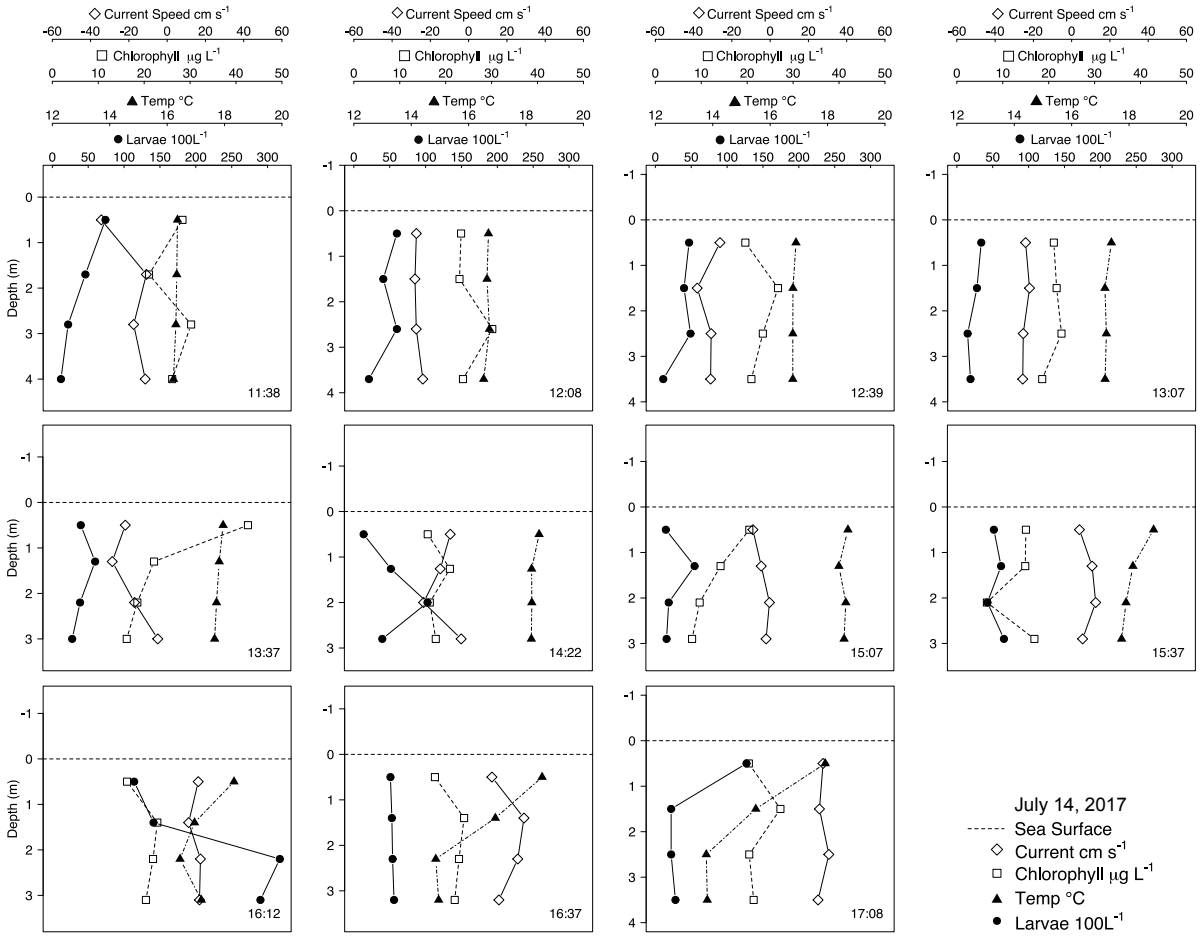

Figure 6. Field samples collected on July 14, 2017 in Fidalgo Bay. Each plot shows one sampling event, which includes samples collected at four depths beginning at the time listed in the bottom right corner. Black circles represent the number of larvae collected in 100L of pumped water, gray triangles show the water temperature (°C), white squares represent the chlorophyll-*a* (µg L^{-1}), and white diamonds represent current velocity (cm s^{-1}). Negative values of current velocity indicate water moving out of the bay (ebb tide) and positive values indicate water moving into the bay (flood tide). The horizontal dotted line represents the sea surface, which adjusts accordingly so the bottom of each plot represents the seafloor.

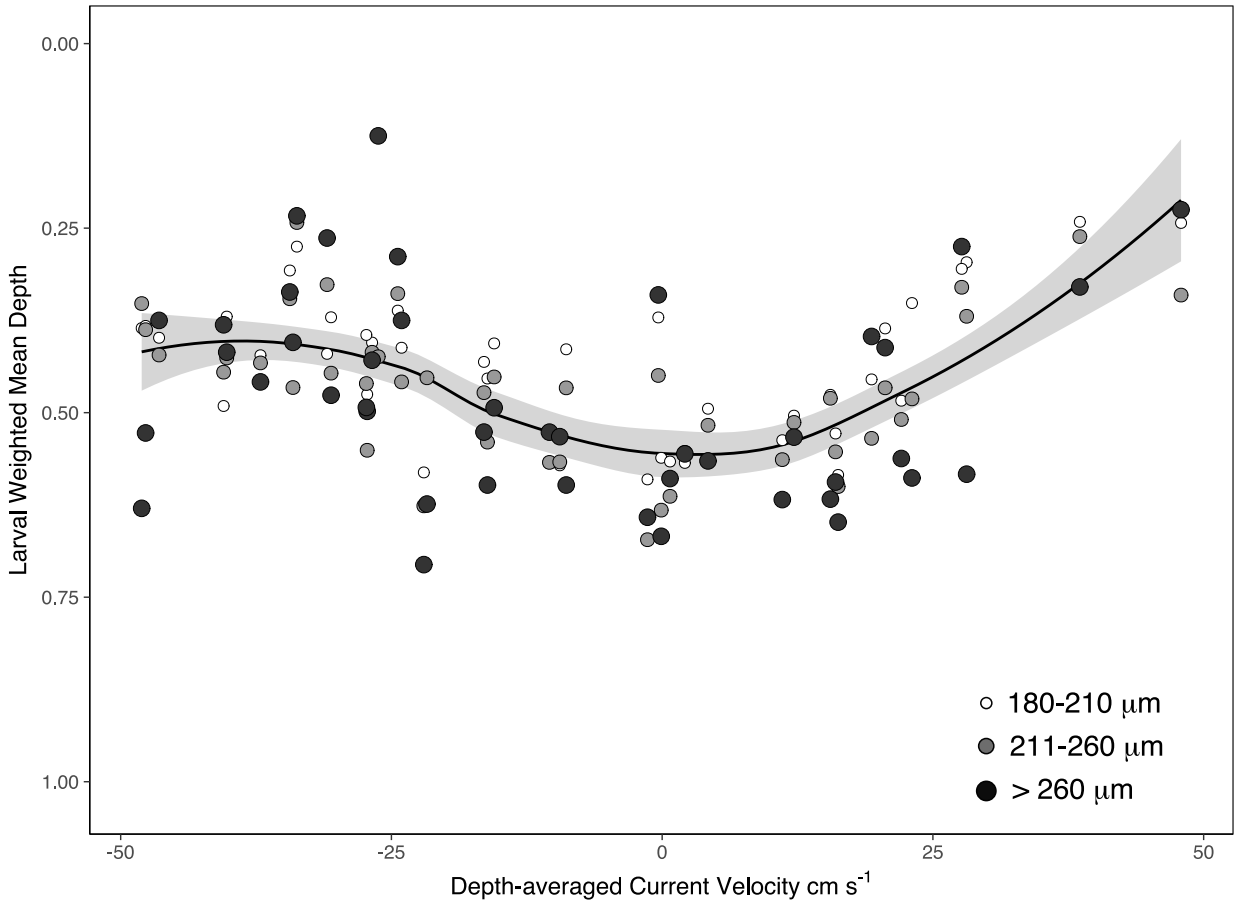

Figure 7. Normalized larval weighted mean depth (WMD) as a function of depth-averaged current velocity (cm s^{-1}) fit with generalized additive modelling thin plate regression spline smoother for all larvae size-classes combined. Shading represents 95% confidence intervals. The size of the plotting circle represents a corresponding larval size-class, which are newly-released (180-210μm), developing (211-260μm), and late-stage (>260μm).

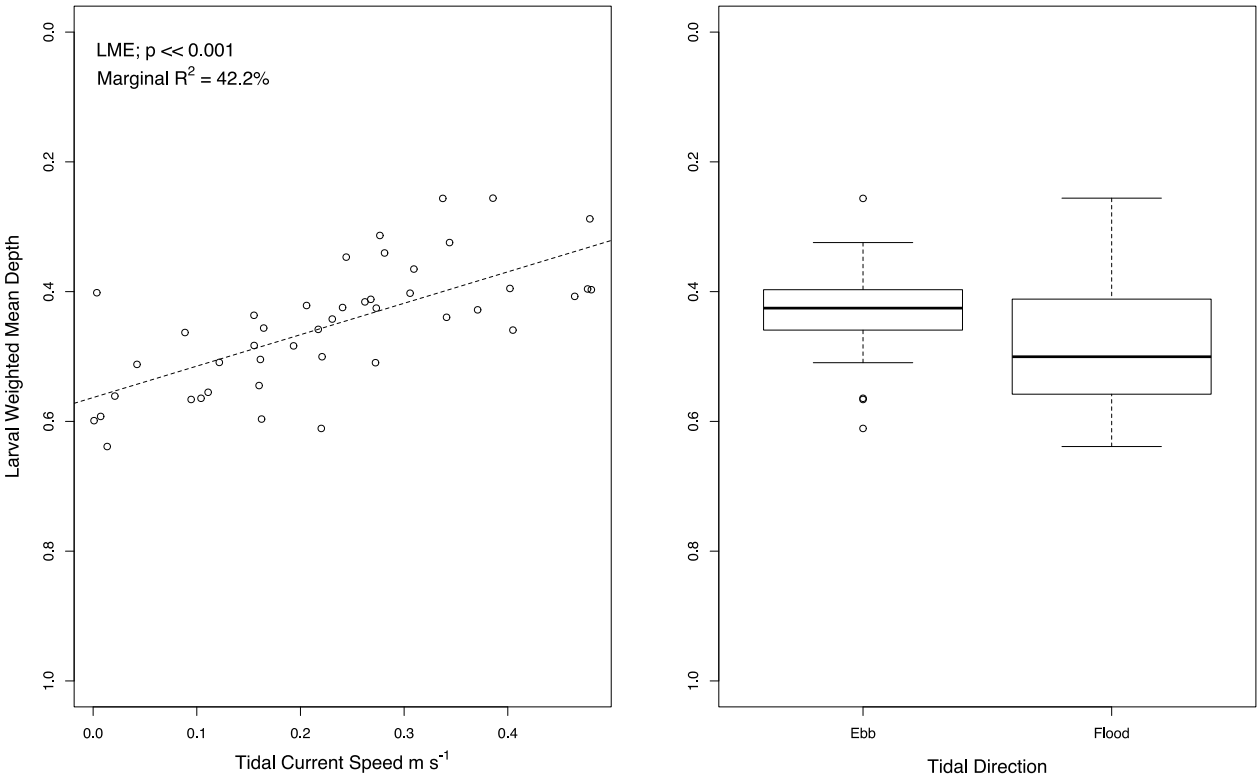

Figure 8. Normalized larval weighted mean depth (A) versus absolute tidal current speed (cm s^{-1}) fitted by linear mixed effect modelling and (B) versus ebb and flood tidal direction. Linear mixed effects modelling results indicate a significant linear relationship between larval WMD and current speed (LME, T = -4.87, $p \ll 0.001$) and no significant effect of tidal direction (LME). A simple pairwise contrast confirms no significant difference between ebb and flood larval WMD ($t_1 = 0.80$, $p = 0.43$).

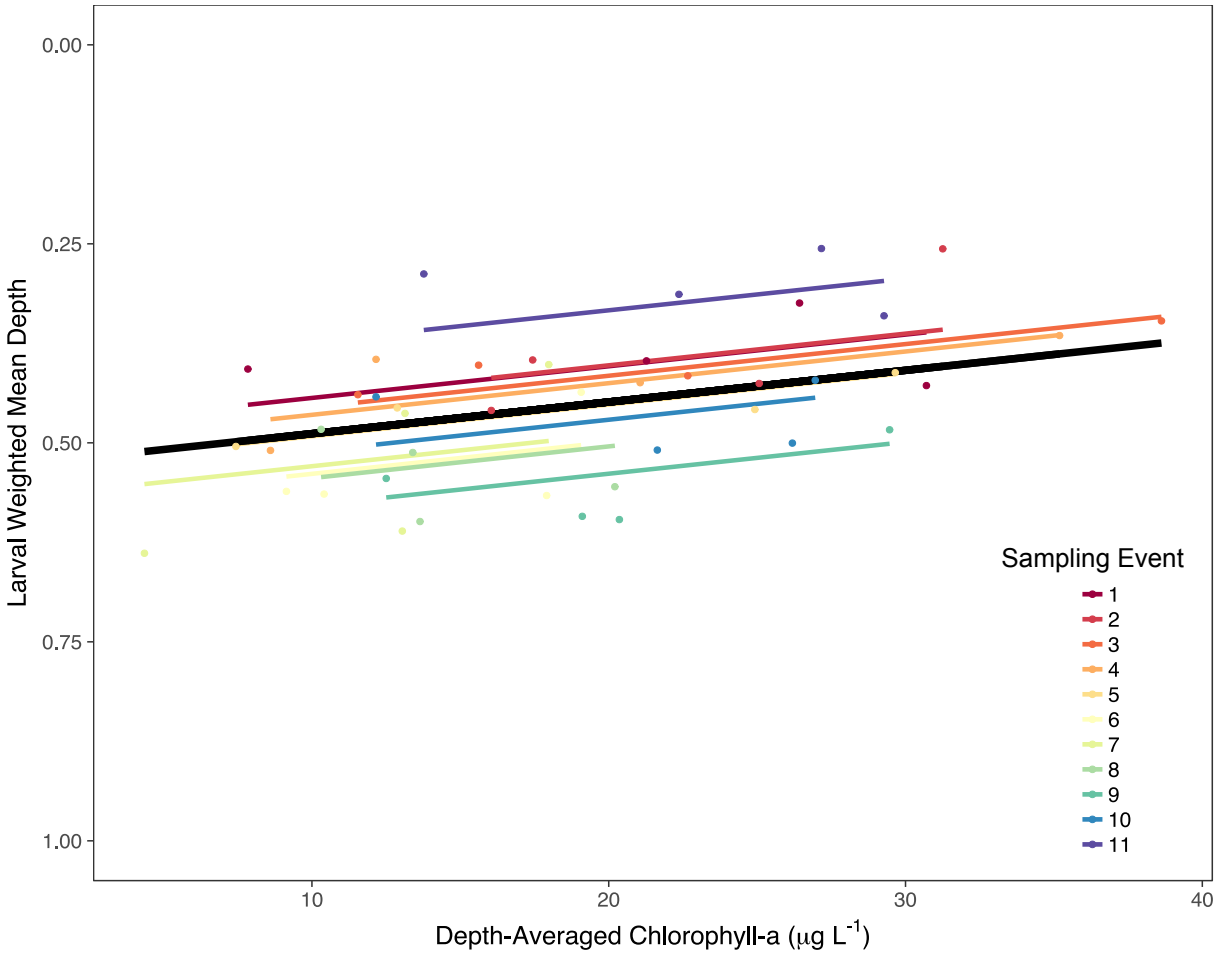

Figure 9. Normalized larval weighted mean depth (WMD) becomes significantly shallower as depth-averaged chlorophyll-*a* (μg L^{-1}) increases (LME, T=-3.8, p≪ 0.001, Table 2). Colored lines represent the model fit for each 'sampling event', which were allowed unique intercepts within the random modeling component of the LME. The thick black line represents the average model fit of the fixed depth-averaged chlorophyll-*a* modeling component of the LME.

Appendix A

Appendix A includes figures displaying the results and validation plots for the statistical models we used for data analysis.

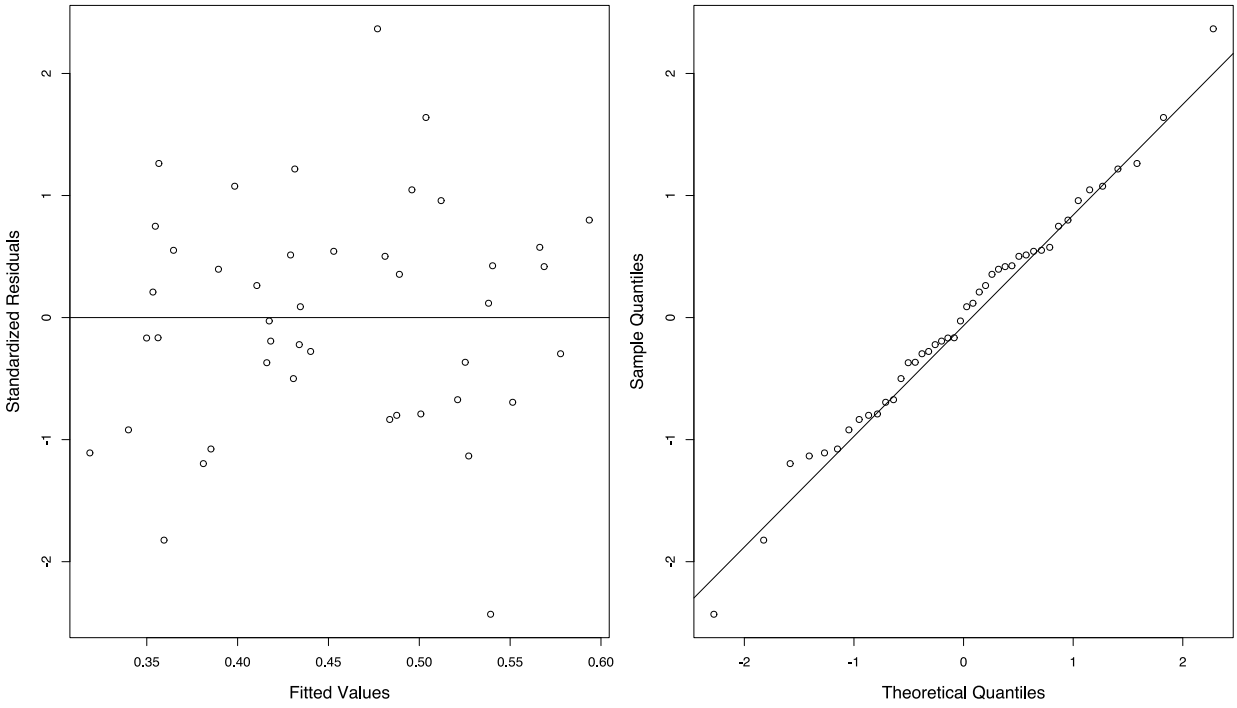

Figure A1. Model validation plots for the final linear mixed effects model predicting larval abundance. The normalized residual plot shows no apparent pattern, which indicates homogeneity in the residuals. The QQ-norm plot indicates some slight violations of normality, but not enough to be concerning for the final model.

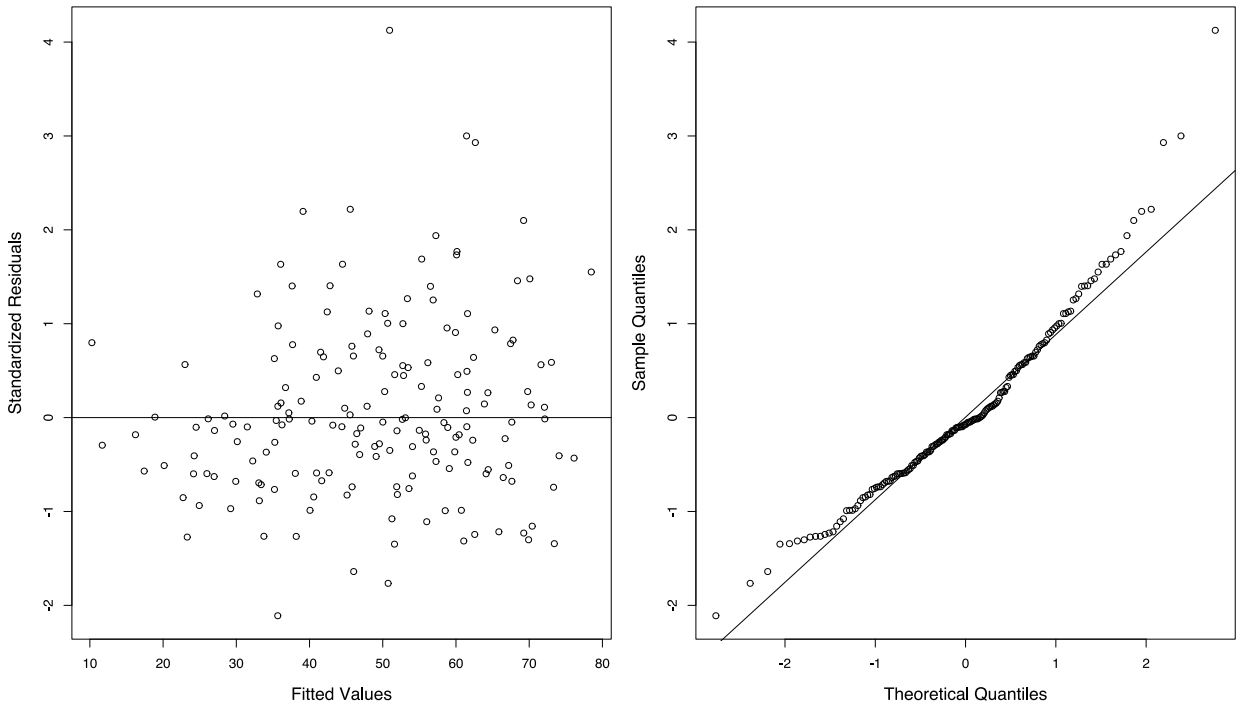

Figure A2. Model validation plots for the final linear mixed effects model predicting larval weighted mean depth. The normalized residual plot shows no apparent pattern, which indicates homogeneity in the residuals.

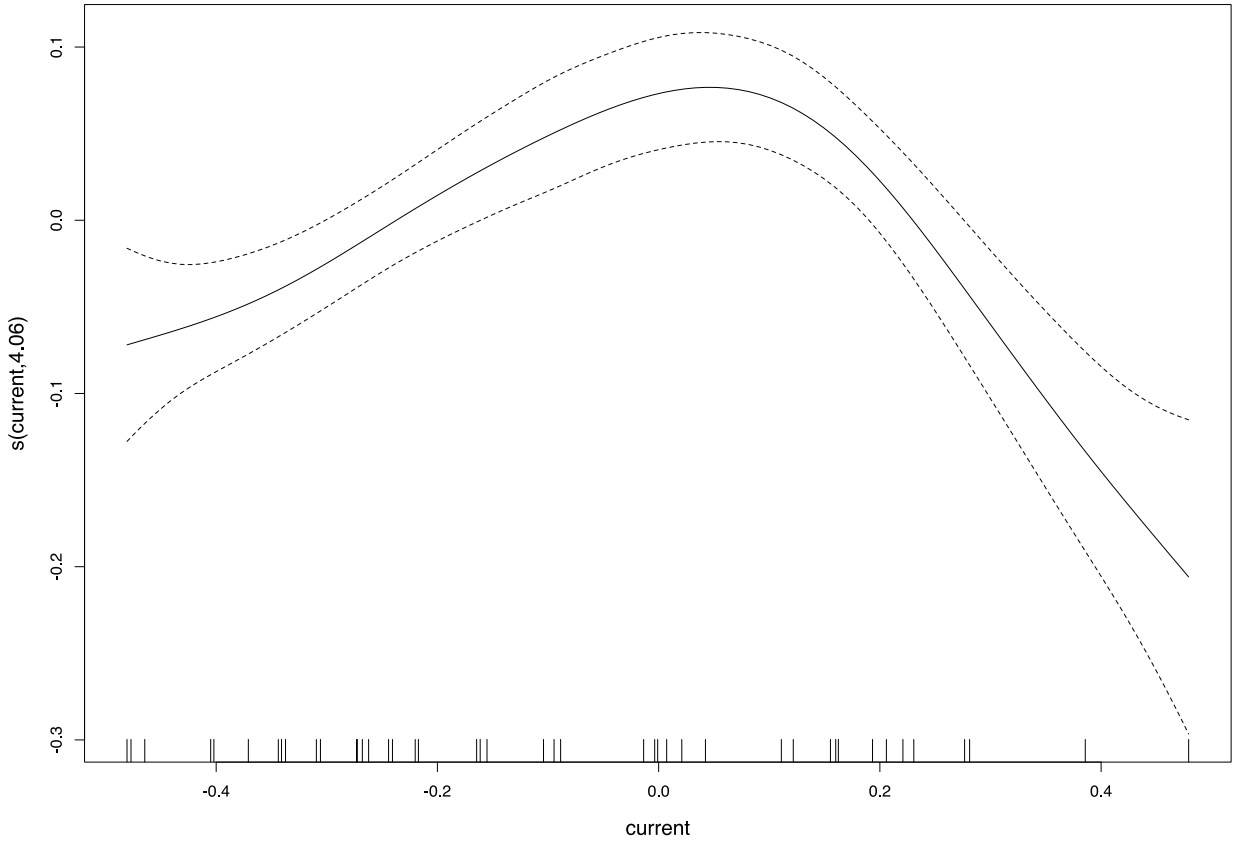

Figure A3. Generalized additive mixed model results showing the partial effect of depth-averaged current velocity (m s^{-1}) on larval WMD (GAMM, $F_{est.4.06} = 11.74$, $p << 0.001$). The y-axis indicates the contribution of the thin plate regression spline smoother to the fitted values. Dotted lines indicate 95% confidence intervals around the smoother and vertical tick marks along the x-axis indicate the current velocity values of each observation.

References

Andrews, J.D. 1983. Transport of bivlave larvae in James River. Journal of Shellfish Research 3: 29–40.

Baker, P., and R. Mann. 2003. Late stage bivalve larvae in a well-mixed estuary are not inert particles. Estuaries 26: 837–845. doi:10.1007/BF02803342.

Barile, P.J., A.W. Stoner, and C.M. Young. 1994. Phototaxis and vertical migration of the queen conch (*Strombus gigas linne*) veliger larvae. Journal of Experimental Marine Biology and Ecology 183. Elsevier: 147–162. doi:10.1016/0022-0981(94)90084-1.

Bayne, B.L. 1964. The responses of the larvae of *Mytilus edulis L.* to light and gravity. Oikos 48: 162–174.

Beck, M.W., R.D. Brumbaugh, L. Airoldi, A. Carranza, L. D. Coen, C. Crawford, O. Defeo, et al. 2011. Oyster Reefs at Risk and Recommendations for Conservation, Restoration, and Management. BioScience. doi:10.1525/bio.2011.61.2.5.

Blake, B., and A. Bradbury. 2012. Washington Department of Fish and Wildlife Plan for Rebuilding Olympia Oyster (*Ostrea lurida*) Populations in Puget Sound with a Historical and Contemporary Overview. Brinnon, WA: Washington State Department of Fish and Wildlife.

Bartoń, K. 2017. MuMIn: Multi-Model Inference. R package version 1.40.0. https://CRAN.R-project.org/package=MuMIn

Carriker, M.R. 1951. Ecological Observations on the Distribution of Oyster Larvae in New-Jersey Estuaries. Ecological Monographs 21: 19–38.

Carson, H.S. 2010. Population connectivity of the Olympia oyster in southern California. Limnology and Oceanography 55: 134-148.

Civelek, C.V., R.M. Daigle, and A. Metaxas. 2013. Effects of temperature on larval swimming patterns regulate vertical distribution relative to thermoclines in *Asterias rubens*. Journal of Experimental Marine Biology and Ecology 445. Elsevier B.V.: 1–12. doi:10.1016/j.jembe.2013.03.010.

Cowen, R.K., and S. Sponaugle. 2009. Larval Dispersal and Marine Population Connectivity. Annual Review of Marine Science 1: 443–466. doi:10.1146/annurev.marine.010908.163757.

Daigle, R.M., and A. Metaxas. 2011. Vertical distribution of marine invertebrate larvae in response to thermal stratification in the laboratory. Journal of Experimental Marine Biology and Ecology 409. Elsevier B.V.: 89–98. doi:10.1016/j.jembe.2011.08.008.

Dekshenieks, M.M., E.E. Hofmann, J. M. Klinck, and E. N. Powell. 1996. Modeling the vertical distribution of oyster larvae in response to environmental conditions. Marine Ecology Progress Series 136: 97–110. doi:10.3354/meps136097.

Dinnel, Paul. 2016. Restoration of the Native Oyster , *Ostrea lurida* , in Fidalgo Bay , Padilla Bay and Cypress Island Year Fourteen Report.

Dinnel, P., B. Peabody, and T. Peter-Contesse. 2009. Dinnel et al 2009. Journal of Shellfish Research 28: 79–85.

Dobretsov, S.V., and G. Miron. 2001. Larval and post-larval vertical distribution of the mussel *Mytilus edulis* in the white sea. Marine Ecology Progress Series 218: 179–187. doi:10.3354/meps218179.

Dyer, Keith R. 1997. Estuaries: a physical introduction. 2nd ed. Chichester: Wiley & Sons.

Finelli, C.M., and D.S. Wethey. 2003. Behavior of oyster (*Crassostrea virginica*) larvae in flume boundary layer flows. Marine Biology 143: 703–711. doi:10.1007/s00227-003-1110-z.

Fox, J. and S. Weisberg. 2011. An {R} Companion to Applied Regression, Second Edition. Thousand Oaks CA: Sage. URL: http://socserv.socsci.mcmaster.ca/jfox/Books/Companion

Fuchs, H.L., E.J. Hunter, E.L. Schmitt, and R.A. Guazzo. 2013. Active downward propulsion by oyster larvae in turbulence. The Journal of experimental biology 216: 1458-1469.

Fuchs, H.L., G.P. Gerbi, E.J. Hunter, A.J. Christman, and F.J. Diez. 2015. Hydrodynamic sensing and behavior by oyster larvae in turbulence and waves. Journal of Experimental Biology 218: 1419–1432. doi:10.1242/jeb.118562.

Gallager, S.M., J.L. Manuel, D.A. Manning, and R. O'Dor. 1996. Ontogenetic changes in the vertical distribution of giant scallop larvae, *Placopecten magellanicus*, in 9-m deep mesocosms as a function of light, food, and temperature stratification. Marine Biology 124: 679–692. doi:10.1007/BF00351049.

Garrison, L.P., and J.A. Morgan. 1999. Abundance and vertical distribution of drifting, post-larval *Macoma spp.* (Bivalvia: Tellinidae) in the York River, Virginia, USA. Marine Ecology Progress Series 182: 175–185. doi:10.3354/meps182175.

Gibson, R.N. 2003. Go with the flow: Tidal migration in marine animals. Hydrobiologia 503: 153–161. doi:10.1023/B:HYDR.0000008488.33614.62.

Gross, T.F., F.E. Werner, and J. E. Eckman. 1992. Numerical modeling of larval settlement in turbulent bottom boundary layers. Journal of Marine Research 50: 611-642.

Hidu, H., and H.H. Haskin. 1978. Swimming speeds of oyster larvae *Crassostrea virginica* in different salinities and temperatures. Coastal and Estuarine Research Federation 1: 269–276.

Jonsson, P.R., C. Andre, and M. Lindegarth. 1991. Swimming Behavior of Marine Bivalve Larvae in a Flume Boundary-Layer Flow-Evidence for near-Bottom Confinement. Marine Ecology Progress Series 79: 67–76. doi:10.3354/meps079067.

Kim, C.K., K. Park, S.P. Powers, W.M. Graham, and K.M. Bayha. 2010. Oyster larval transport in coastal Alabama: Dominance of physical transport over biological behavior in a shallow estuary. Journal of Geophysical Research: Oceans 115: 1–16. doi:10.1029/2010JC006115.

Levin, Lisa. 2006. Larval dispersal: recent progress in understanding new directions and digressions. Integrative and Comparative Biology 46: 282-297.

Lloyd, M.J., A. Metaxas, and B. DeYoung. 2012. Patterns in vertical distribution and their potential effects on transport of larval benthic invertebrates in a shallow embayment. Marine Ecology Progress Series 469: 37–52. doi:10.3354/meps09983.

Loosanoff, V.L., H.C. Davis, and P.E. Chanley. 1966. Dimensions and shapes of larvae of some marine bivalve mollusks. Malacologia 4: 351–435.

López-Duarte, P.C., and R. A. Tankersley. 2009. Developmental shift in the selective tidal-stream transport behavior of larvae of the fiddler crab *Uca minax* (LeConte). Journal of Experimental Marine Biology and Ecology 368: 169-180.

Mann, R. 1988. Distribution of bivalve larvae at a frontal system in the James River, Virginia. Marine Ecology Progress Series 50: 29–44. doi:10.3354/meps050029.

Manuel, J.L, S.M. Gallager, C.M. Pearce, D.A. Manning, and R.K. O'Dor. 1996. Veligers from different populations of sea scallop *Placopecten magellanicus* have different vertical migration patterns. Marine Ecology Progress Series 142: 147–163. doi:10.3354/meps142147.

Metaxas, A., and C.M. Young. 1998. Responses of echinoid larvae to food patches of different algal densities. Marine Biology 130: 433–445. doi:10.1007/s002270050264.

Miller, S.H., and S.G. Morgan. 2013. Phenotypic plasticity in larval swimming behavior in estuarine and coastal crab populations. Journal of Experimental Marine Biology and Ecology 449. Elsevier B.V.: 45–50. doi:10.1016/j.jembe.2013.08.013.

Morgan, S.G., J.L. Fisher, S.T. McAfee, J.L. Largier, S.H. Miller, M.M. Sheridan, and J.E. Neigel. 2014. Transport of Crustacean Larvae Between a Low-Inflow Estuary and Coastal Waters. Estuaries and Coasts 37: 1269–1283. doi:10.1007/s12237-014-9772-y.

Murphy, K., L. Dominguez, and B. Bookheim. 2008. Fidalgo Bay Environmental Aquatic Reserve Management Plan. Aquatic Reserves Program Washington State Department of Natural Resources. https://www.dnr.wa.gov/publications/aqr_rsve_fid_mgmt_plan.pdf

Nakagawa, S. and H. Schielzeth.2013. A general and simple method for obtaining R2 from generalized linear mixed-effects models. Method in Ecology and Evolution 4: 133–142.

Narváez, D.A., J.M. Klinck, E.N. Powell, E.E. Hofmann, J.Wilkin, and D.B. Haidvogel. 2012. Modeling the dispersal of eastern oyster (*Crassostrea virginica*) larvae in Delaware Bay. Journal of Marine Research 70: 381–409. doi:10.1357/002224012802851940.

North, E.W., Z. Schlag, R.R. Hood, M. Li, L. Zhong, T. Gross, and V.S. Kennedy. 2008. Vertical swimming behavior influences the dispersal of simulated oyster larvae in a coupled particle-tracking and hydrodynamic model of Chesapeake Bay. Marine Ecology Progress Series 359: 99–115. doi:10.3354/meps07317.

O'Connor, M.I., J.F. Bruno, S.D. Gaines, B.S. Halpern, S.E. Lester, B.P. Kinlan, and J.M. Weiss. 2007. Temperature control of larval dispersal and the implications for marine ecology,

evolution, and conservation. Proceedings of the National Academy of Sciences 104: 1266–1271. doi:10.1073/pnas.0603422104.

Peteiro, L., and A. Shanks. 2015. Up and down or how to stay in the bay: Retentive strategies of Olympia oyster larvae in a shallow estuary. Marine Ecology Progress Series 530:103-117.

Pinheiro J., D. Bates, S. DebRoy, D. Sarkar and R Core Team (2017). nlme: Linear and Nonlinear Mixed Effects Models_. R package version 3.1-131, <URL: https://CRAN.R-project.org/package=nlme>.

Pritchard, C., A. Shanks, R. Rimler, M. Oates, and S. Rumrill. 2015. The Olympia Oyster *Ostrea lurida* : Recent Advances in Natural History, Ecology, and Restoration. Journal of Shellfish Research 34: 259-271. doi:10.2983/035.034.0207.

Raby, D., Y. Lagadeuc, J.J. Dodson, and M. Mingelbier. 1994. Relationship between feeding and vertical distribution of bivalve larvae in stratified and mixed waters. Marine Ecology Progress Series 103: 275–284.

R Core Team. 2016. R: A language and environment for statistical computing. R Foundation for Statistical Computing, Vienna, Austria. <URL: https://www.R-project.org/.

Sameoto, J.A., and A. Metaxas. 2008. Interactive effects of haloclines and food patches on the vertical distribution of 3 species of temperate invertebrate larvae. Journal of Experimental Marine Biology and Ecology 367: 131–141. doi:10.1016/J.JEMBE.2008.09.003.

Scyphers, S.B., S.P. Powers, K.L. Heck, and D. Byron. 2011. Oyster reefs as natural breakwaters mitigate shoreline loss and facilitate fisheries. PLoS ONE. doi:10.1371/journal.pone.0022396.

Shanks, Alan L. 2001. An identification guide to the larval marine invertebrates of the Pacific Northwest. Oregon State University Press, Corvallis, OR.

Shanks, A.L., and L. Brink. 2005. Upwelling, downwelling, and cross-shelf transport of bivalve larvae: Test of a hypothesis. Marine Ecology Progress Series 302: 1–12. doi:10.3354/meps302001.

Steele, E.N. 1957. The rise and decline of the Olympia oyster. Fulco Publications, Elma, WA.

Thomas, Y., F. Dumas, and S. Andréfouët. 2014. Larval dispersal modeling of pearl oyster *Pinctada margaritifera* following realistic environmental and biological forcing in Ahe Atoll lagoon. PLoS ONE 9. doi:10.1371/journal.pone.0095050.

Tremblay, M.J., and M.M. Sinclair. 1988. The vertical and horizontal distribution of sea scallop (*Placopecten magellanicus*) larvae in the Bay of Fundy in 1984 and 1985. Journal of Northwest Atlantic Fisheries Science 8: 43-53.

Warnes, G.R., B. Bolker, T. Lumley, and R.C. Johnson. 2015. 2015. gmodels: Various R Programming Tools for Model Fitting. R package version 2.16.2. https://CRAN.R-project.org/package=gmodels

Welch, J., and R. Forward. 2001. Flood tide transport of blue crab, *Callinectes sapidus*, postlarvae: Behavioral responses to salinity and turbulence. Marine Biology 139: 911–918. doi:10.1007/s002270100649.

Wheeler, J.D., K.R. Helfrich, E.J. Anderson, B. McGann, P. Staats, A.E. Wargula, K. Wilt, and L.S. Mullineaux. 2013. Upward swimming of competent oyster larvae *Crassostrea virginica* persists in highly turbulent flow as detected by PIV flow subtraction. Marine Ecology Progress Series 488: 171-185.

Wheeler, J.D., K.R. Helfrich, E.J. Anderson, and L.S. Mullineaux. 2015. Isolating the hydrodynamic triggers of the dive response in eastern oyster larvae. Limnology and Oceanography 60: 1332–1343. doi:10.1002/lno.10098.

Winter, Bodo. 2014. A very basic tutorial for performing linear mixed effects analyses (Tutorial 2). Archives of environmental contamination and toxicology: 1–22.

Wood, S.N. 2011. Fast stable restricted maximum likelihood and marginal likelihood estimation of semiparametric generalized linear models. Journal of the Royal Statistical Society (B) 73: 3-36.

Wood, L., and W.J. Hargis. 1971. Transport of bivalve larvae in a tidal estuary. In Fourth European Marine Biology Symposium, Bangor, September 1969, ed. D. J. Crisp, 29–44. Cambridge: Cambridge University Press.

Young, C.M. 1995. Behavior and locomotion during the dispersal phase of larval life. In Ecology of Marine Invertebrate Larvae, ed. L. R. McEdward, 249–277. Boca Raton, FL: CRC Press.

zu Ermgassen, P.S.E., M.W. Gray, C.J. Langdon, M.D. Spalding, and R.D. Brumbaugh. 2013. Quantifying the historic contribution of Olympia oysters to filtration in Pacific Coast (USA) estuaries and the implications for restoration objectives. Aquatic Ecology 47: 149–161. doi:10.1007/s10452-013-9431-6.

Zuur, A.F., E.N. Ieno, N.J. Walker, A.A. Saveliev, and G.M. Smith. 2009. Mixed Effects Models and Extensions in Ecology with R. Edited by M. Gail, K. Krickeberg, A. Tsiatis, W. Wong, and J. Samet. New York: Springer Science+Business Media. doi:10.1007/978-0-387-87458-6.